Final Report on NASA Grant
NGR 50-002-215

An Investigation of Surface Albedo Variations During the Recent Sahel Drought

Carl C. Norton, Frederick R. Mosher,
and Barry Hinton

(NASA-CR-157448) AN INVESTIGATION OF SURFACE ALBEDO VARIATIONS DURING THE RECENT SAHEL DROUGHT Final Report (Wisconsin Univ.) 58 p HC A04/MF A01 CSCL 04A

N79-29727

Unclas
G3/46 31756

Space Science and Engineering Center
University of Wisconsin
Madison, WI 53706

ABSTRACT

Applications Technology Satellite (ATS) III green sensor data are used to measure surface reflectance variations in the Sahara/Sahel during the recent drought period; 1967 to 1974. The magnitude of the seasonal reflectance change is shown to be as much as 80% for years of normal precipitation and less than 50% for drought years. Year to year comparisons during both wet and dry seasons reveal the existence of a surface reflectance cycle coincident with the drought intensity. The relationship between the green reflectance and solar albedo is examined and estimated to be about 0.6 times the reflectance change observed by the green channel.

1. Introduction

The hardships imposed by the extended drought on the inhabitants of the African Sahel and Sudan focused scientific attention on the problem of desert encroachment and drought. There is mounting evidence to support the idea that the desertification is caused to a large extent by the very people who suffer the consequences. This is not a new theory. The influence of the agricultural and herding practics of man on desertification in semi-arid regions was pointed out by Lowdermilk (1935) and Stebbing (1937) nearly a half-century ago. More recently Bernus (1974) supports this idea with his study of population movements in the Sahel.

Recent investigators have related the sub-desert drought to meteorological causes such as: shifting of the sub-tropical high pressure belt, Lamb (1973); expansion of the circumpolar vortex, Winstanley (1973): increase in atmospheric aerosols and carbon dioxide, Bryson (1973); and changes in the southern hemisphere meridional temperature gradient, Kraus, (1977). Since the Sahelian rainfall is governed almost exclusively by the migration of the inter-tropical convergence zone (ITCZ) (Aspliden and Adefololu, 1976, Ilesanmi, 1971, Kelley, 1975), these parameters must in some manner be related to its fluctuation. The exact cause-effect relationship, however, is not clear.

2. Albedo influence on precipitation-numerical modelling

The numerical modelling results of recent studies have provided a plausible link between man and rainfall in semi-arid regions such as the Sahel. The most noticeable effect of man and his animals on the subdesert environment is the altered surface albedo. Charney (1975)

contends that the destructive agricultural techniques utilized and the browsing of livestock denudes the vegetation, causing an increase in the surface albedo. The increased albedo results in a net radiative loss which produces general subsidence and drying over the area, thereby inhibiting or reducing the convection necessary for rain.

The geophysical aspect of Charney's mechanism was examined by Charney, Quirk, Chow, & Kornfield (1977) using the Goddard Institute of Space Science (GISS) Global Circulation Model (GCM). Their numerical modelling demonstrated that a significant reduction in precipitation could be achieved by increasing the Sahel albedo from .14 to .35. They also found, however, that changes in the evaporation rate could be just as important as albedo changes. This is a very significant point. Idso and Deardorff (1978) and Berkofsky (1978) point out the dangers involved in considering only the albedo variation aspect of altered ground cover.

Similarly, Berkofsky (1976) used a modified version of a tropical numerical model to calculate the vertical motion at the top of the boundary layer as a function of the surface albedo. He made calculations for the northern Negev desert in June and December 1974. He found that sinking motion was associated with high albedoes with a gradual reversal of the vertical motion as surface albedo was decreased.

Otterman (1974) studied the effects of baring high albedo soils in the Sinai-Negev region. He found a sharp contrast between the bright Sinai and the relatively dark Negev along an erected fence line. Close surface observations of the area revealed that on the Sinai side the soil had been denuded of vegetation by overgrazing and destruction of inedible vegetation by Bedouin herds while on the protected Negev side there were few

herds and natural vegetation was relatively abundant. Airborne radiometer measurements showed the bright side to be 5°C cooler during the day in August. Measurements by a hand held radiometer showed the bright side to be 3.5°C cooler in February. Satellite thermal imagery of the area showed the Sinai to be cooler but no quantitative evaluation was made. Otterman proposed that the "thermal depression" in the Sinai could result in reduced convection and therefore reduced rainfall in the area.

Jackson and Idso (1975) measured surface albedoes and temperatures in the southwestern United States desert for several years. They also found that the surface albedo and temperature were related; but in the reverse sense that Otterman found. They suggested that the result of denuding would be a warmer surface.

3. Purpose of Study

The purpose of our study was to examine the surface albedo variations in and around the Sahel during the period 1967 through 1974. We wished to determine the magnitude of the seasonal albedo changes as well as any year to year variations for the same season. We also wished to investigate the relationship between albedo and precipitation patterns. We anticipated that an albedo-rainfall relationship would be most pronounced in the semi-arid areas where plant life is almost totally dependent on seasonal rainfall. Thus we believed that some correlation of precipitation and albedo might be observed in the Sahel with some appropriate lead or lag time. For convenience we use the word "albedo" to refer to the percent reflectance as detected by the green sensor (.48 - .58 μm range) of the ATS III satellite. All measurements were made using data from this sensor.

4. Data Selection

The measurements of surface albedoes over the Sahara-Sahel during the period of interest could only be accomplished with satellite data. There are several characteristics of the satellite data set to be used that are highly desirable: 1. It should be complete so that relatively cloud-free data may be selected; 2. The data should lend itself to accurate satellite to earth coordinate transformation (earth location) so that identical areas may be compared; 3. The sensor should be calibrated, or a known albedo reference point should be available in each day's data; 4. The resolution should be sufficiently high to permit exclusion of clouds from the surface albedo measurements; 5. The sensor sensitivity should be constant or change linearly; 6. The satellite viewing angle should be constant; 7. The sensor response range should include the solar spectrum. No satellite possesses all of these characteristics, however, the ATS III has all but the last; and to some extent the fourth. First, we will examine the sensor resolution problem.

Although the ATS III camera has a satellite subpoint resolution of 3.5 km, a resolution problem exists because the instantaneous field of view over west Africa encompasses a 5 km by 7 km area. Any clouds the order of this size could not be detected and certainly small cumuli would be undetectable on the displayed data.

The problem of small cloud contamination was investigated using a simulation study. It was assumed that small cloud contamination would be due to randomly distributed individual cumulus clouds. Software was developed roughly along the same lines as the simulation study done by Shenk and Salomonson (1972) to produce theoretical histograms assuming: typical ATS III brightness values for cloud (54) and surface

ORIGINAL PAGE IS
OF POOR QUALITY

(16), cloud size (1 km^2), and sensor scan area (36 km^2) while varying the percent cloud coverage. In each case 100 samples were generated. Figure 1. shows a histogram of simulated sensor response to an area with 20% cloud cover. In all cases of cloud coverage greater than 10%, there was no occurrence of the surface brightness value on the histogram. At 10% cloud cover the modal value was 19 while at 30% it increased to 29. Thus it appears that increasingly large errors in albedo measurements will exist as the small cloud coverage increases beyond 10%. This contamination probably is most serious in the southern area of the Sahel where small cumuli are more prevalent.

Now we will consider the limited sensor response range of the ATS III. To better understand the significance of our observations in the context of climatic change, we need to consider the probable relationship of the observed albedo change in the green, to the corresponding change in the solar spectral band as a whole. Figure 2 shows the approximate distribution of solar radiation incident on the earth's surface after transmission through a relatively dry atmosphere. The same figure also indicates the spectral distribution of the green channel sensitivity. One can see that, although the peaks of these two curves fall roughly at the same wavelength, the green channel samples only a small fraction of the total (~.131).

Curve A of Figure 3 is a synthetic reflectance profile of a healthy dark green leaf, modelled after published results (see Reeves, 1975, and references therein) and unpublished data (Polcyn, 1968). According to Fresnels laws, the many interfaces between air, cellulose and water, all differing in refractive index, make the leaf a scattering medium. This accounts for the high reflectance between 0.75 and 1.3 μm where absorption

is absent. The decreasing reflectivity for longer wavelengths is due almost entirely to the absorption bands of the included water. Leaves contain chlorophyll and other pigments, which absorb wavelengths shorter than 0.75 μm, but between 0.52 and 0.56 μm a gap in absorption allows green reflection, resulting in the familiar green color of most plants.

As moisture is reduced to the point of stress the absorption beyond 1.2 μm, due to water, diminishes. The production of pigments also diminishes, allowing increased reflection in the visible and loss of the characteristic green peak. Thus, the dark green plants become a light "dry" brown color as shown in curve B of Figure 3. In Figure 4 the spectral distribution of reflected solar radiation for both a healthy green, and a dry brown leaf are shown.

Leaves are relatively opaque in the visible, however from 0.75 to 1.3 μm, relatively high leaf transparency, may allow the soil to be partially seen through the leaves. In the case of sparse vegetation, the soil may also be exposed to view directly. Consequently, we must consider the reflective properties of soils, as we are particularly concerned with sparse vegetation in this paper.

There is a great variety to the possible reflective properties of soils. Fortunately most soils contain mixtures of minerals which tend to reduce the importance of specific molecular absorption bands. Generally, soils are brown. That is, they exhibit an increasing reflection from violet through red. Curve A of Figure 5 represents fairly well typical reflectance of dry light red-brown sand.

Soil reflective properties are affected by factors apart from composition, such as particle size, aggregation of particles into larger

structures, surface roughness and superficial or absorbed water. Coarse particles, or aggregates of particles form a porous surface full of holes and voids which act as "black bodies" or perfect absorbers. Very fine particles tend to fill voids producing an even or uniform surface of higher reflectivity. Consistent with visual observations, it has been established that across the solar spectrum wet soils reflect less than dry soils. This is partly due to absorption by water, but also partly from a reduction in scattering caused by the water film filling gaps between soil particles, and effectively reducing the number of scattering interfaces. Curve B of Figure 5 represents the wet reflectivity of the same soil as Curve A. For more information on soil reflectivity see Reeves (1975) and references therein.

Figure 6 shows the spectral distribution of reflected solar radiation for these models of wet and dry soils. The two curves of Figure 4 and the two curves of Figure 6 can be used as a first approximation to a complete set of functions to estimate the observed spectra of reflected radiation in natural scenes. This may be done by adding the components together in different fractional proportions. Then, one can integrate over the spectrum to obtain the mean albedo for solar radiation, or multiply by the spectral distribution of sensitivity of the ATS III green channel before integration and obtain estimates of the corresponding albedo which would be observed by the green sensor. Table 1 shows the results for a few significant cases. In Figure 7 we have plotted these to show the covariance of green and solar albedo.

Values in the vicinity of points labeled 2 and 2B in Figure 7 should correspond to typical observations during a normal wet season when plants

are green. During a normal dry season, or in early stages of drought observed values will migrate toward 3 and 4. As devegetation proceeds values may decrease again, but only slightly, toward 4, 5 and 5A. Points labeled 1, 6, 6A, 6B and 7 represent values which would be observed just after a rain under prior conditions indicated by the originating points of the arrows. Two conclusions can be drawn from the table and from Figure 7. First, the transition from healthy green vegetation to dry vegetation produces a marked albedo change. Secondly, the further transition from dry vegetation to no vegetation probably does not produce an easily detectable albedo change. To the extent one can rely on the model reflectivities, the slope of the curve of Fig. 7 indicates that the reflectivity change from the green channel alone probably overestimates the average change over the solar spectrum. Observed changes should be multiplied by a factor of about 0.6 to improve the estimate.

5. Data Processing

The ATS III data was available as hard copy pictures and digital tapes. The pictures represented the most complete data set, but their use was ruled out because of the non-quantitative nature of photographic data. A search through the available digital tape archive revealed that apparently cloud free data were available for at least one day of the years 1967, 1969, 1972, 1973, & 1974 during the dry season (winter); and for 1969, 1972, 1973, & 1974 during the rainy season (summer). We assumed that the data for each day was representative of the season for that year. We believed this data set was adequate to depict the progress of any albedo changes.

The data were earth located to insure that the same areas were compared. Although the data were selected because they were the most

cloud free, it was desirable to further reduce the cloud cover in some cases. This was made possible through use of a minimum brightness composite (Mosher, 1977). The process consisted of superimposing several digital areas from different days at similar solar zenith angles and selecting the minimum brightness value for each data point to construct a composite area. This process efffectively removed visible clouds everywhere except locations that were cloud contaminated on all data sets.

The data were displayed on the Man-Computer Interactive Data Access System (McIDAS) and brightness measurement made over 2° square areas. This grid was chosen to provide adequate resolution while retaining a sufficiently large number of digital values to retain statistical reliability. By using the draw mode of the area statistics program it was possible to draw around and therefore exclude any visible cloud from the digital values measured in each square. The output consisted of a histogram of brightness values for each square. It was assumed that the mode of each histogram represented the brightness value of the surface in each 2° square area. Attempts to use other values such as the mean or lowest brightness count resulted in inconsistent albedoes.

All of the albedo values were derived assuming isotropic scattering from the various surfaces occurring throughout the area examined. This appears to be a good assumption for sandy desert soils over a large range of solar zenith angles as evidenced by Brennan and Bandeen's (1970) measurements at Carson sink with an airborne medium resolution radiometer. For other types of surfaces the isotropic assumption introduces increasingly large errors as the solar zenith angle increases from local noon. For

this reason, the available data with the smallest solar zenith angles were selected for measurements.

6. Normalization

In order to eliminate gain changes, sensor degradation, and atmospheric contaminants, each data set was normalized with respect to the area located northwest of Timbuktu centered at 19N 05W. This area was chosen because it is one of the brightest areas on the pictures, and is centrally located with respect to the area of investigation. It is an area of minimum statistical cloudiness and is comprised of sand dunes and hard rocky soil with extremely sparce vegetation (Griffiths, 1972). Comparisons of this Saharan normalization point with White Sands, New Mex. and Salar de Uyuni in Bolivia show approximately ±12% variation in albedo.

The Modal brightness value obtained for each square was normalized with respect to the Sahara and the cosine of the solar zenith angle was applied to normalize all data to local noon using the following equation.

$$A = I_o D_m / \cos\Theta \qquad (1)$$

In (1) D_m is the modal brightness value from the histogram, Θ is the solar zenith angle and I_o the normalizing factor from the Sahara normalization point.

It was discovered that a systematic error appeared in the albedoes computed from data with large sun angles. This was due in part to the back scatter of radiation along the increased path length through the atmosphere. It is also probable that the reflectance characteristics of the various

surfaces contributed to the zenith angle dependence of the albedo. (Kalma and Badham, 1972) Unrealistically large values of albedo were computed when the zenith angle increased beyond about 45°.

In order to correct for this effect, albedo measurements were made of identical areas at three times; 1200, 1400, & 1600Z. Using the 1200Z albedoes as "ground truth", the amount by which the brightness values at the other times would have to be decreased to give the 1200Z value was determined and plotted on a graph. (Figure 8) On the same graph the theoretical increase due to Rayleigh scattering from Coulson, Dave, Sekera, (1960) for surface albedoes of .25 & .80 were plotted along with values obtained by Rockwood & Cox (1976). A correction curve was then drawn considering all of the plotted data. Corrections derived from this curve were then applied to all computed albedoes with solar zenith angles greater than 20°.

7. Estimated Error of Albedo Measurement

In order to obtain an estimate of the error involved in our surface albedo measurement technique we computed the mean albedoes and standard deviations for each 2° square in the Sahara (19°N to 23°N) for all the data sets. We then divided the individual standard deviations by the respective mean albedoes to obtain an error estimate for each square. The mean of these individual estimates was then taken to represent the error in the measurement technique. A value of 11% was determined for the total data set. Accordingly the error in the values labelled percent difference is twice as large or 22%. Therefore the albedo change isopleths with values of 25% or greater are significant.

8. Results

a. Surface Albedo Maps

Surface albedo measurements were made for 19 Nov. 1967, 15 Sept. 1969, 6 Jan. 1970, 19 July 1972, 13 Dec. 1972, 23 Dec. 1972, 14 Aug. 1973, 19 Oct. 1973, 2 July 1974, and 21 Sept. 1974. The pattern of albedoes over the area shows similar features for all the data. (Figures 9-18) Note carefully that these figures all refer to green channel albedo. The band of high albedoes extending from northeast Mali through central Mauritania is common to all the charts as is the Saharan relative albedo minimum located near the northern border of Mauritania and Mali. The lines of constant albedo generally parallel the mean isohyets in the Sahel. Most of the data show an albedo gradient that is primarily latitudinal with the largest gradient occurring between 15°N and 19°N. The exceptions, 13 Dec. 1972 and 14 Aug. 1973, show a pronounced east-west albedo gradient in the south central Sahel.

The 23 Dec. 1972 albedo measurements presented an enigma. Although the analysis of this data showed the same general features as the other analyses, the albedoes were much lower in the southeastern Sahel than they were on 13 Dec. Attempts to account for the anomalously low (.14 to .12) values were inconclusive. Satellite photographs of the area suggest that broad scale rain may have occurred in the southern Sahel during the intervening 10 day period. It is difficult to believe that vegetation could respond so quickly, however, the reduced albedoes could be due to the altered reflective characteristics of the wetted soil as discussed in Section 4. The data for this day were excluded from all presentations.

b. Comparison With Another Albedo Study

A comparison of our surface albedo patterns derived from ATS III data with those derived by Rockwood and Cox (1976) using SMS data for 1974 shows a reasonably good correlation. The differences between the sets of albedo measurements may be due to the different wavelength sensitivities of the sensors used, i.e., .48 to .58 μm for the ATS III and .55 to .75 μm for SMS. Our measurements were made at 1300Z on 2 July and 1500Z on 21 September. Their measurements were at 1200Z on 2 July and 20 September. It is not surprising that the July data sets agree more closely than the September data since the former sets are separated by only one hour. In the July data our albedos over the Sahara are approximately the same as those of Rockwood and Cox, but to the south our values are somewhat higher. Our .35 albedo line approximates their .31 line. For the September data, our values are lower in the Sahara but about the same to the south. The general features described earlier appear in both data sets for the two days.

c. Sahelian Albedo Changes

In order to examine the overall Sahelian surface albedo changes, the area was subdivided into a Saharan area, 18 to 22° N, and a Sahelian area 12 to 18° N. The data were subdivided into a wet season set consisting of 15 Sept. 1969, 19 July 1972, 14 Aug. 1973, and 21 Sept. 1974; and a dry season set consisting of 19 Nov. 1967, 06 Jan. 1970, 13 Dec. 1972, 19 Oct. 1973, and 2 July, 1974. The inclusion of the July, 1974 data in the dry set and the July, 1972 data in the wet set is justified by the differences in the northward rainfall progression in the two years. More correctly, the area south of 14°N in the July, 1974 data should be considered wet

season while the remainder of the area is dry season.

A mean albedo for the Sahara and the Sahel was computed for each data set. Since we assumed the Sahara remained constant during the entire period, we computed a mean albedo for the Sahara for all data sets. We then obtained a normalization factor for each mean Sahelian albedo by dividing the Saharan value for each data set by the mean Saharan value of all the data sets. This normalization process reduces the random noise in the albedo measurement technique. These normalized mean albedos for the entire Sahel are shown on Figure 19. A smooth curve can be drawn through the data points if we neglect 23 Dec. 1972. The curves for both wet and dry seasons show an increase in the albedos through 1973 followed by a decrease in 1974. Note that the albedo difference between the wet and dry season is relatively large in the beginning of the drought and that the wet season albedo approaches the dry season value during the height of the drought. The dry season albedo increase over the entire Sahel is approximately 20% while the wet season increase is approximately 50%.

d. Seasonal albedo change

Our data clearly depicted the obvious rainfall-albedo variation between the wet and dry season in the Sahel. We found a relaxed albedo gradient in the dry season and a strong gradient in the wet season; as did Rockwood and Cox (1976). The mean latitudinal albedoes averaged between 16°W and 0°W for July, 1974 (dry season) and September, 1974 (wet season) showed relative changes of 0% at -11°N, -14% at 13°N, -25% at 15°N, -30% at 17°N, and -5% at 19°N, and 21°N. This compares well with the values found by Rockwood and Cox. (Figure 20)

The map of albedo change for 1974 (Figure 21) shows a larger relative

change in the western Sahel as compared with the Eastern Sahel. This may be due to the greater rainfall experienced in June 1974 in the eastern Sahel. The seasonal change between September 1969 and January 1970 revealed a similar (but reversed) pattern of albedo changes with about the same magnitude of the 1974 seasonal change (Figure 22). The relative albedo increase averaged along 15° N was 50%; i.e., from .18 to .27. The changes for 13, 17, and 19° N were 30, 28, and -03% respectively. The largest albedo increase occurred along the Atlantic coast near the Senegal-Mauritania border and along 15° N in the central Sahel. The maximum change for any 2° square was approximately 100%; i.e., from .15 to .30. Seasonal albedo changes for 1972 and 1973 (Figures 23-24) did not show patterns similar to the 1969 and 1974 albedo changes or comparable magnitudes of albedo change. The 1972 seasonal change shows maximum increases of 50% occurring in southern Senegal where possible cloud contamination was present in the dry season data. The 1973 albedo changes occur in the central Sahel and amount to 25% increases. We believe the reduced seasonal change of albedo during the 1972-1973 period to be a result of the drought.

e. Inter-Annual Albedo

The interannual variation of surface albedo was examined for both the wet season and the dry season. For the wet season the percentage albedo change for three time intervals were examined: September, 1969 to July, 1972 (Figure 25); September, 1969 to August, 1973 (Figure 26); and September, 1969 to September, 1974 (Figure 27). September 1969 was selected as a

basis of comparison because the 1969 wet season was generally normal in the Sahel. The maximum albedo increases are approximately the same as the maximum observed for the seasonal variation, approximately 100%. The albedo increases for all three intervals show a similar pattern, however, the values are slightly higher for the 1969-1972 and 1969-1973 intervals, possibly reflecting the return toward normalcy with the increased 1974 wet season rains.

The dry season albedo change patterns are not as regular in shape or as large as the wet season. (Figures 28-31) Albedo changes between November 1967 and January 1970 are mostly within the noise limits of the measurements. This lack of change is to be expected since both years experienced more or less normal rainfall. The November 1967 to October 1973 albedo change maps show areas of larger percent changes to occur in southeast Senegal, south Mali, and Upper Volta. The changes are slightly larger for the 1967 to 1973 period than for the 1967 to 1972 period, perhaps reflecting the increased intensity of the drought in 1973. The November 1967 to July 1974 albedo change maps show the largest increases (30-40%) are farther north, extending along a line similar to the wet season change pattern. The lower albedo changes south are probably due to the rain that fell in the southern Sahel in June. The November 1973 to July 1974 100 mm isohyet extends approximately along 13° N across the Sahel. Generally more than 75% of the rain during this period fell in June.

f. Albedo and Precipitation

In order to attempt to relate albedo and precipitation, we compiled

annual rainfall data from the WMO monthly summaries for all stations throughout the southern Sahara, Sahel, and tropical rainy areas. The precipitation for all stations in the 2° square areas was averaged and plots made for each year of the precipitation vs. the albedo during the following dry season. Not surprisingly, the higher albedo boxes were generally associated with low precipitation and vice versa for most years. The correlation coefficients for 1967, 1969, 1972, 1973, and 1974 were -.57, -.45, -.58, .07, and -.72 resp. Only the 1974 correlation was significant at the 1% level. A comparison of the 19 Oct. 1973 albedo with the mean precipitation from 1967 through 1973 gave a correlation of -.43; not significant at the 5% level. The latitudinal means of albedo and precipitation showed no significant correlation. Similarly the changes of mean latitudinal albedo and precipitation were uncorrelated.

In attempting to determine whether a causative relationship existed between the precipitation of one year and the albedo of either the preceding or following year, several plots of precipitation vs. albedo were made. The results were as shown in table 2.

9. Conclusions

The satellite inferred green channel reflectance measurements indicate the existence of a surface albedo cycle for both the wet and dry seasons during the 1967 to 1974 Sahel drought (Figure 19). The mean dry season reflectance for the Sahel increased from .29 in 1967 to .34 in 1973. The wet season data showed an increase from .23 in 1969 to .33 in 1973. The estimated error in the surface green channel reflectance measurements is ±11% of the measured values. It appears that as the drought progressed the wet season surface reflectance approached that of the normal dry season.

This trend was also pointed out by the seasonal reflectance change data (Figures 21-24). Seasonal reflectance variations of as much as 80% were found in the Central Sahel during years of normal precipitation while the variation for drought years generally amounted to less than 50%. In order to estimate the total solar albedo changes, the green channel values shown in figures 09 through 18 should be multiplied by a factor of 0.6 (Fig. 7).

The proposition that increased albedoes produce subsequent rainfall deficits remains unproven. One of the two cases examined showed some degree of correlation of the 1973 dry season albedo with the 1974 precipitation. The second case showed no correlation between the 1972 dry season albedo and the 1973 precipitation. The two cases used to examine the reverse relationship were similarly contradictory.

Acknowledgements. We wish to thank Gary Chatters for his invaluable assistance in resurrecting the ATS digital data processing technique. This research was supported by National Aeronautics and Space Administration grant number NGR50-002-215.

References

Aspliden, C. I. and D. Adefololu, 1976: The Mean Troposphere of West Africa. J. Appl. Meteor., 7, 705-716.

Berkofsky, L., 1976: The Effect of Variable Surface Albedo on the Atmospheric Circulation in Desert Regions. J. Appl. Meteor., 15, pp. 1139-1144.

_____, 1978: Reply. J. Appl. Meteor., 17, p. 561.

Bernus, E., 1974: Une\Tribu Touoregue Sohelienne et son aire de Nomadisation. Paris, O.R.S.T.O.M., 116 pp.

Brennan, B. and W. R. Bandeen, 1970: Anisotropic Reflectance Characteristics of Natural Earth Surfaces. Appl. Opt. 9, pp. 405-412.

Bryson, R. A., 1973: Climatic Modification by Air Pollution, II: The Sahelian Effect, Institute for Environmental Studies, Rep. 9, University of Wisconsin, Madison, 12 p.

Charney, J. G., 1975: Dynamics of deserts and drought in the Sahel. Quar. J. Roy. Met. Soc., 101, No. 438, p. 193-202.

Charney, J., W. J. Quirk, S. Chow, and J. Kornfield, 1977: A Comparative Study of the Effects of Albedo Change on Drought in Semi-Arid Regions. J. Atmos. Sci., 34, 1366-1385.

Coulson, K. L., J. V. Dave, and Z. Sekera, 1960: Tables Related to Radiation Emerging From a Planetary Atmosphere with Rayleigh Scattering. Berkeley and Los Angeles, University of California Press, 548 pp.

Griffiths, J. F., 1972: Climates of Africa. World Survey of Climatology, H. Landsberg, ed., 10, Elsevier Publ. Co., Amsterdam, 604 p.

Idso, S. B. and J. W. Deardorff, 1978: Comments on "The Effect of Variable Surface Albedo on the Atmospheric Circulation in Desert Regions". J. Appl. Meteor., 17, p. 560.

Ilesanmi, O. O, 1971: An empirical formulation of an ITD rainfall model for the tropics: A case study for Nigeria. Jour. Appl. Met. 10 (5): 882-891.

Jackson, R. P. and S. B. Idso, 1975: Surface Albedo and Desertification. Science, 189, 1012-1013.

Kalma, J. D. and R. Badham, 1972: The Radiation Balance of a Tropical Pasture, I. The Reflection of Short-Wave Radiation. Agric. Meteorol. 10: 251-259.

Kelley, T. J., 1975: Climate and the West African Drought, Drought, Famine, and Population Movements in Africa. J. L. Neuman, ed., Maxwell School of Citizenship and Public Affairs, Syracuse University, 144 pp.

Kraus, E. B., 1977: Subtropical Droughts and Cross-Equatorial Transports. Mon. Wea. Rev., 105, 1052-1055.

Lamb, H. H., 1973: Some comments on atmospheric pressure variations in the northern hemisphere, Drought in Africa. Center for African Studies, University of London, pp. 27 & 28.

Lowdermilk, W. C. 1935: Man Made Deserts. Pacific Affairs, 8, pp. 409-419.

Mosher, F. R., 1977: Studies of Soundings and Imaging Measurements. Space Science and Engineering Center, University of Wisconsin, Madison, pp. 111-126.

Nicholson, S. E., 1976: A Climatic Chronology for Africa: Synthesis of Geological, Historical, and Meteorological Information and Data. Ph.D. Thesis, University of Wisconsin, pp. 324.

Otterman, J., 1974: Baring high-albedo soils by overgrazing: A hypothesized desertification mechanism. Science, 186, 531-533.

Reeves, R. G., 1975: Manual of Remote Sensing, Vol. I, II, American Society of Photogrammetry, Falls Church, Virginia.

Rockwood, A. A., and S. K. Cox, 1976: Satellite Inferred Surface Albedo Over Northwestern Africa. Atmos. Sci. Pap. No. 265, Colorado State University, 64 pp.

Shenk, W. E. and V. V. Solomonson, 1972: A Simulation Study Exploring the Effects of Sensor Spatial Resolution on Estimates of Cloud Cover From Satellites. J. Appl. Meteor., 11, pp. 214-220.

Stebbing, E. P., 1937: The Threat of the Sahara. J. Roy. African Soc., 36 (supplement), 3-35.

Winstanley, Derek, 1973: Recent rainfall trends in Africa, the Middle East and India. Nature 243: 464-465.

FIGURE LEGEND

Fig. 1. Theoretical histogram resulting from the simulation study.

Fig. 2. Spectral Distribution of Incident Radiation and ATS-3 Green Channel Sensitivity. Curve A represents a 5900K black body with water vapor and CO_2 absorption; B is the green sensitivity. Note that A and B have different units.

Fig. 3. Model Reflectivities for Healthy Dark Green Leaves and Dry Brown Leaves. Curve A is healthy leaf with chlorophyll and water absorption; B represents a dry leaf.

Fig. 4. Spectral Distribution of Radiant Energy Reflected from Leaf Models. The curves of Fig. X2 have been multiplied by the distribution of incident radiation to show the spectral character of radiation reflected by green (curve A) and dry brown (curve B) leaves.

Fig. 5. Spectral Reflectivity Models for Light Red-Brown Sandy Soil. Curve A is the wet state, B the dry state.

Fig. 6. Spectral Distribution of Radiant Energy Reflected Sandy Soil. The curves A and B correspond to A and B respectively of Fig. X4, after multiplication by the spectral distribution of the incident radiation.

Fig. 7. Relationship of Solar Reflectivity and Green Channel Reflectivity. These points are calculated from the model reflectivities. Numerals refer to the corresponding cases in Table 1. Crosses and small numerals have been used for those cases which could only be observed just after a rain and which, therefore, are less probable. Usual wet season observations should lie between 2 and 2B, while normal dry season values would usually be between 3 and 4. Point 5A is the ultimate drought, only dry sand in the scene. For the principal points of the plot (the heavy dots) there is good correlation between green reflectivity and total solar reflectivity. Note, however, that the slope is not one.

Fig. 8. Empirical correction curve used to correct surface albedo measurements made at large solar zenith angles.

Fig. 9. Surface albedoes for Nov. 19, 1967 at 1223 GMT.

Fig. 10. " " " Sept. 15, 1969.

Fig. 11. " " " Jan. 06, 1970.

Fig. 12. " " " July 19, 1972.

TABLE LEGEND

Table 1. Estimates of albedo values for natural scenes of interest composited from synthetic reflectivity curves.

Table 2. Results of precipitation--albedo relationship investigation.

Table 1. Estimates of albedo values for natural scenes of interest composited from synthetic reflectivity curves.

Case Number	Fractional Coeff.* fhl	fdl	fms	fds	Albedo Solar	Green	Surface Character
1	.8	.0	.2	.0	.23	.08	Thick cover, healthy leaves, moist soil
2	.8	.0	.0	.2	.29	.13	Thick cover, healthy leaves, dry soil
3	.0	.8	.0	.2	.48	.43	Thick cover, dry leaves, dry soil
4	.0	.5	.0	.5	.45	.40	Decreased cover, dry leaves, dry soil
5	.0	.2	.0	.8	.42	.38	Thin vegetation, dry leaves, dry soil
6	.0	.2	.8	.0	.19	.18	As 5 but just after rain
7	.0	.8	.2	.0	.42	.38	As 2 but just after rain
7A	1	0	0	0	.26	.07	Very thick healthy vegetation
3A	0	1	0	0	.50	.45	Very thick dry vegetation
6A	0	0	1	0	.11	.11	No vegetation, wet earth
5A	0	0	0	1	.40	.37	No vegetation, dry earth
1B	.5	.0	.5	.0	.19	.09	Like 1, but less cover
2B	.5	.0	.0	.5	.33	.22	Like 2, but less cover
6B	.0	.5	.5	.0	.30	.24	Like 6, but less cover, or 4 after rain

*fhl is fraction of healthy green leaf, fdl the fraction of dry leaves, fms the fraction of moist soil, and fds the fraction of dry soil.

Table 2

Precipitation - Albedo Relationship

precipitation	albedo	correlation coef.
1970	15 Sept 69	-0.26
1969	6 Jan 70	-0.71
1973	13 Dec 72	0.00
1972	19 Oct 73	-0.62
1973	21 Sept 73	-0.15
1974	19 Oct 73	-0.45

Only the 1969 precipitation vs 6 Jan. 1970 correlation is significant at the 1% level.

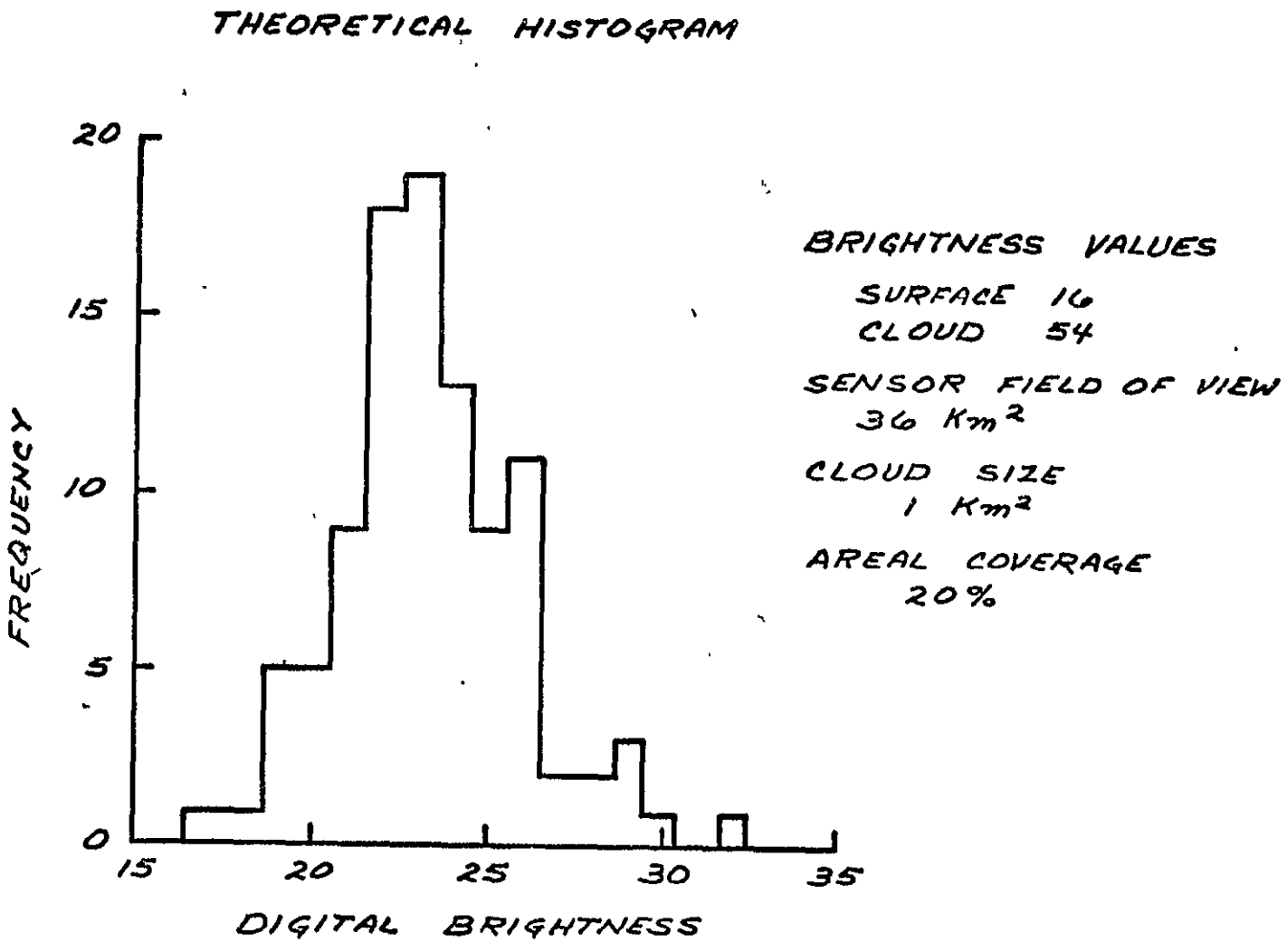

Fig. 1

ORIGINAL PAGE IS
OF POOR QUALITY

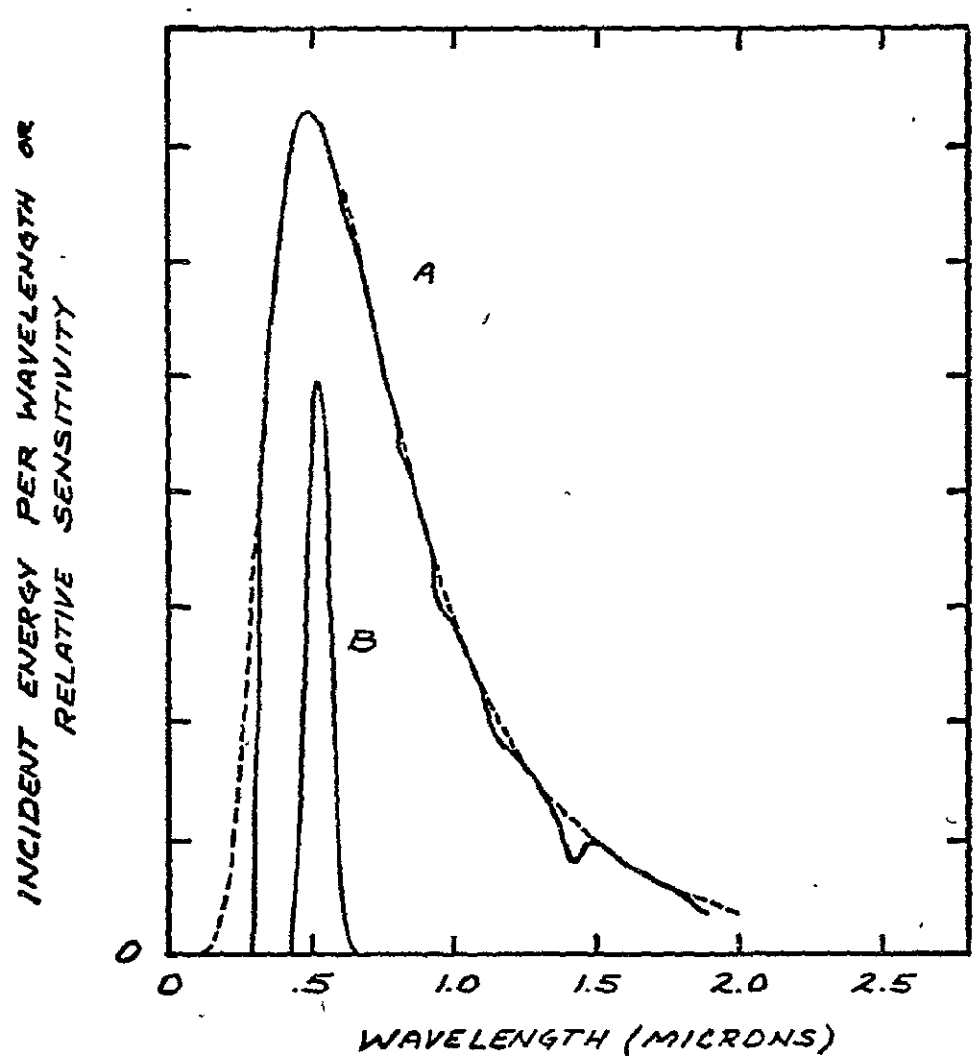
INCIDENT ENERGY PER WAVELENGTH OR
RELATIVE SENSITIVITY
A
B
0
0
.5
1.0
1.5
2.0
2.5
WAVELENGTH (MICRONS)

Fig. 2

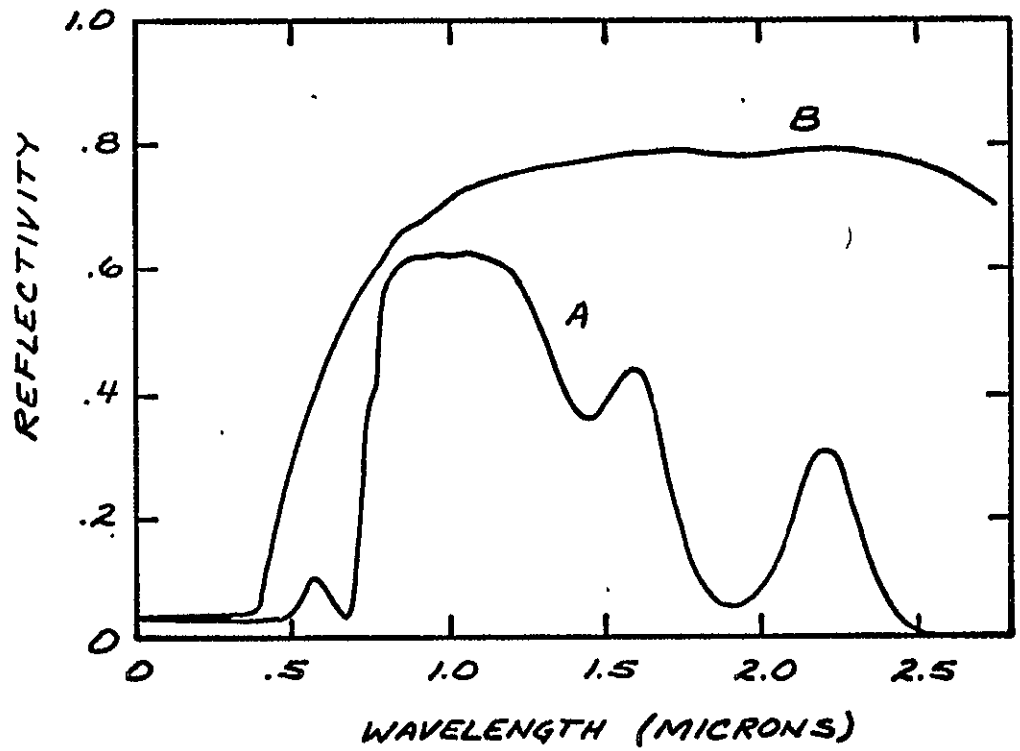

Fig. 3

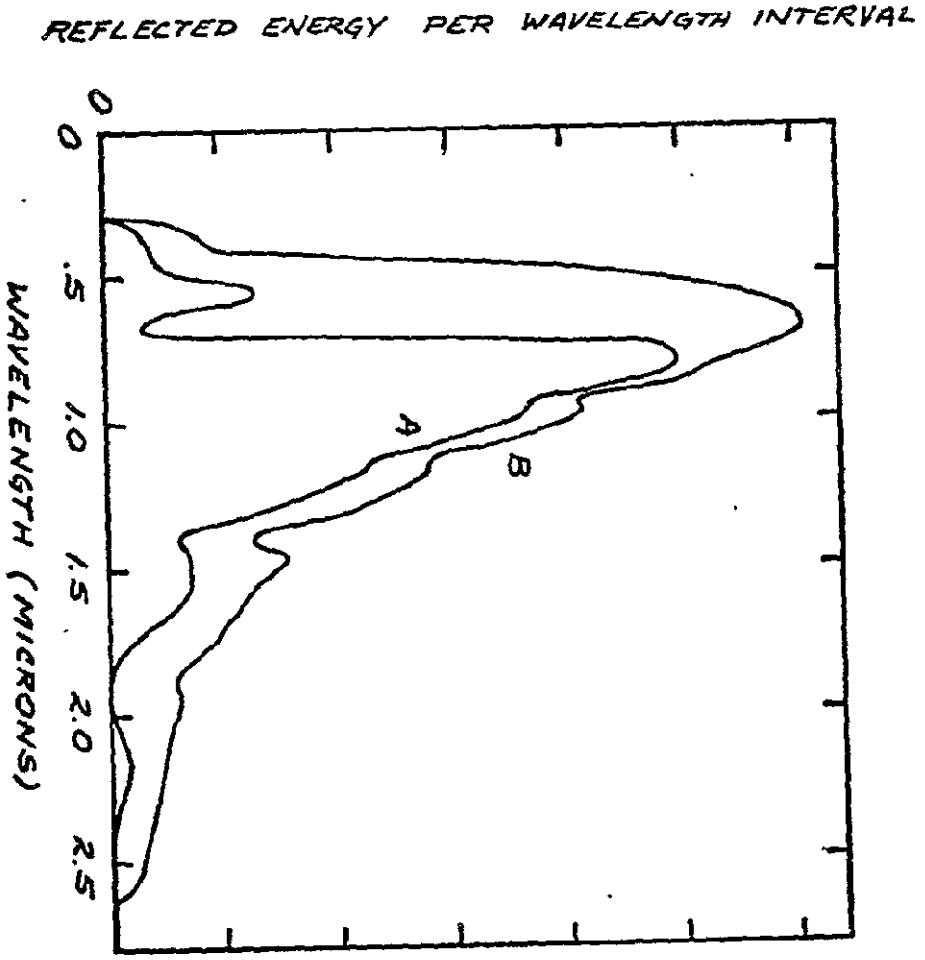
REFLECTED ENERGY PER WAVELENGTH INTERVAL
0
0
.5
1.0
1.5
2.0
2.5
WAVELENGTH (MICRONS)
A
B

Fig. 4

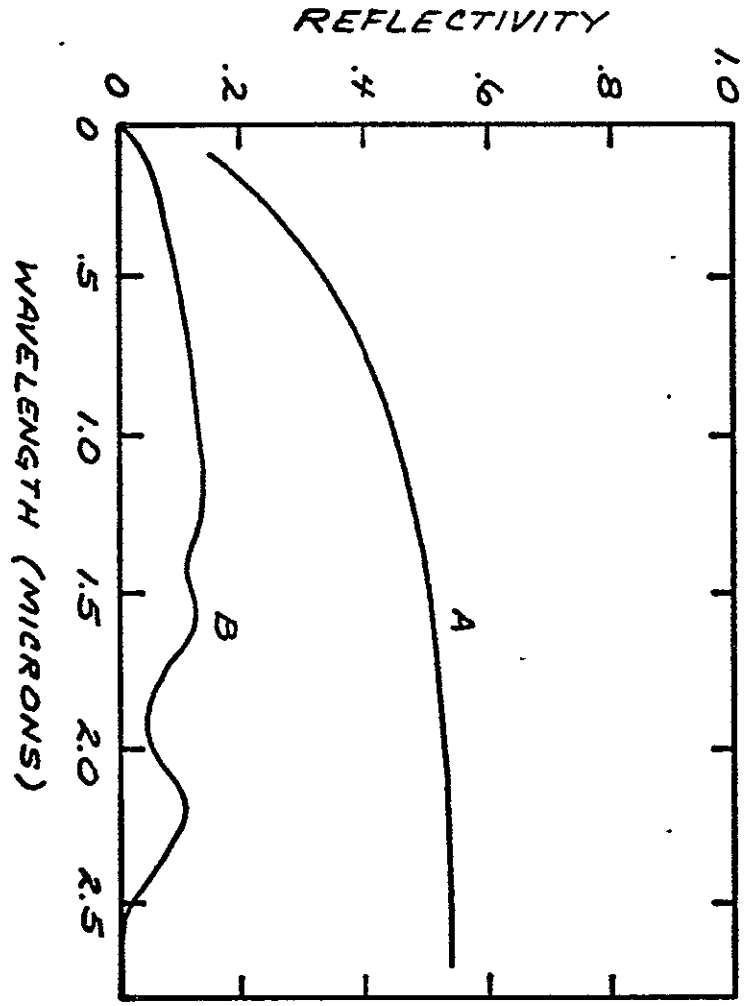

Fig. 5

ORIGINAL PAGE IS
OF POOR QUALITY

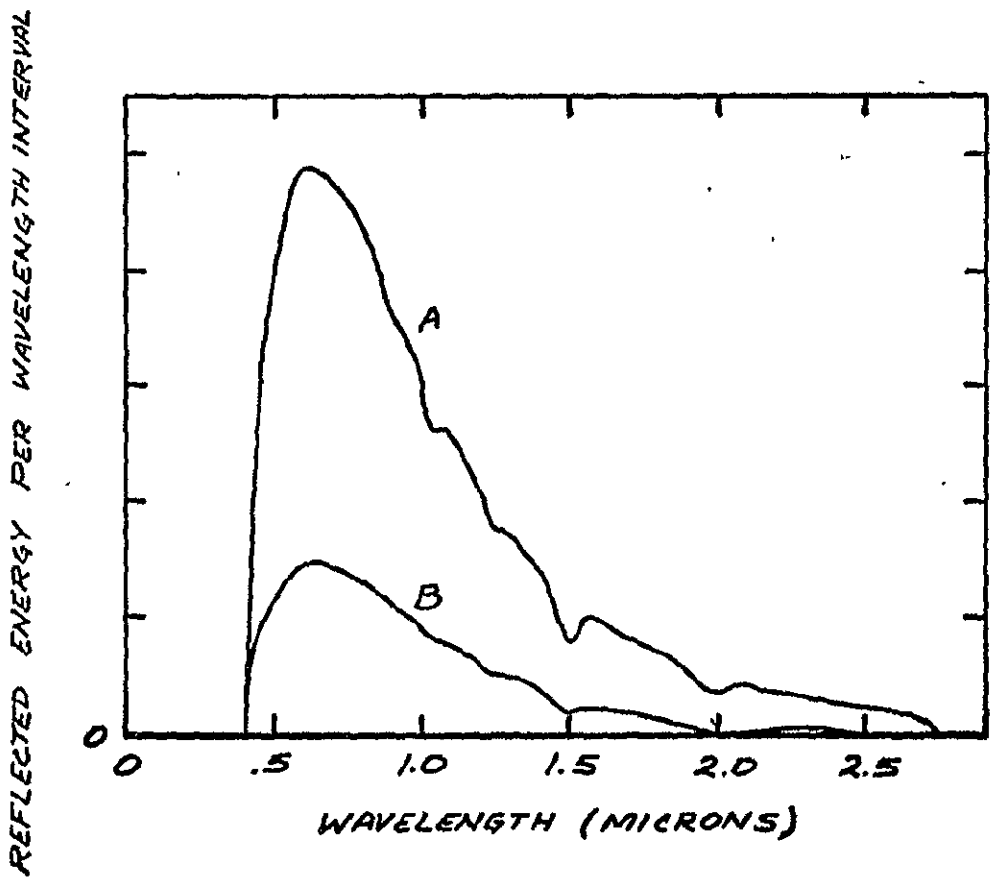
REFLECTED ENERGY PER WAVELENGTH INTERVAL
A
B
0
0
.5
1.0
1.5
2.0
2.5
WAVELENGTH (MICRONS)

Fig. 6

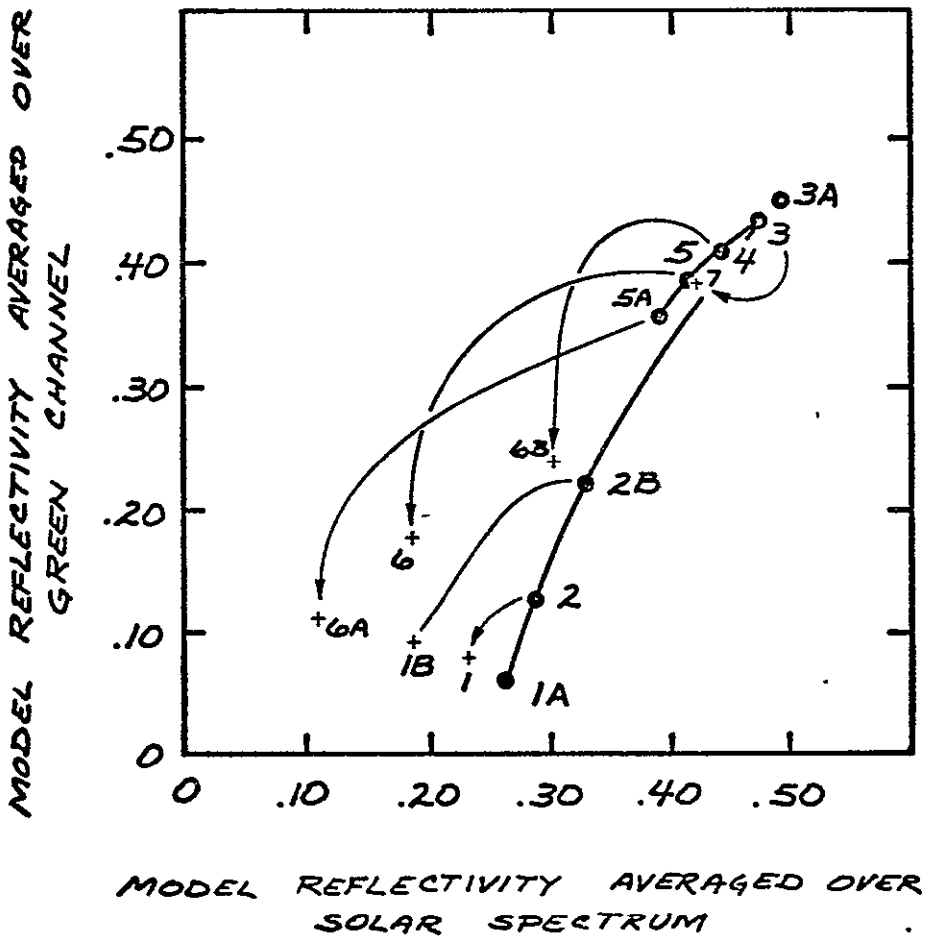
MODEL REFLECTIVITY AVERAGED OVER GREEN CHANNEL
.50
.40
.30
.20
.10
0
0
.10
.20
.30
.40
.50
3A
3
4
5
7
5A
6B
2B
6
6A
2
1B
1
1A
MODEL REFLECTIVITY AVERAGED OVER SOLAR SPECTRUM

Fig. 7

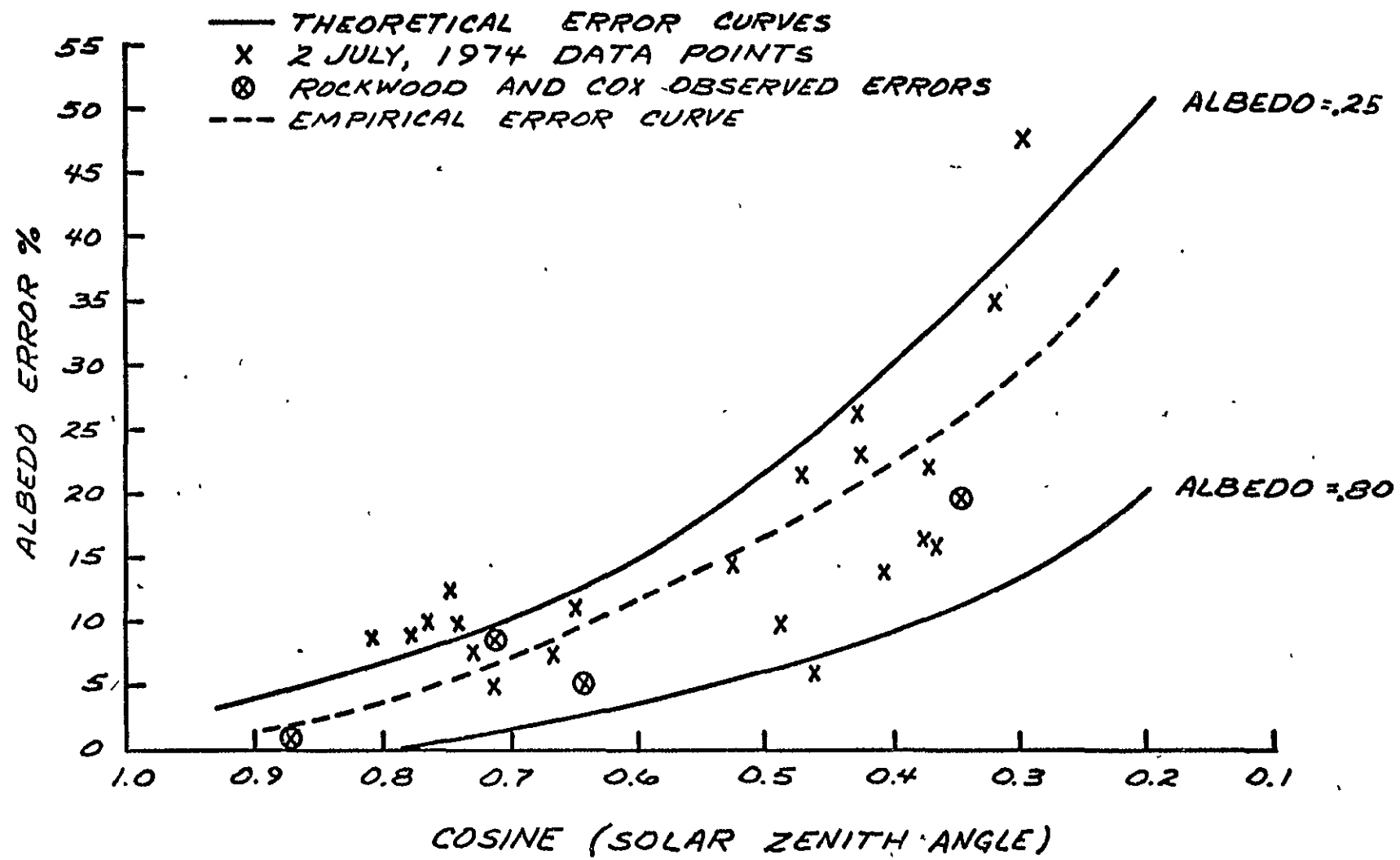
THEORETICAL ERROR CURVES
X 2 JULY, 1974 DATA POINTS
⊗ ROCKWOOD AND COX OBSERVED ERRORS
--- EMPIRICAL ERROR CURVE
ALBEDO =.25
ALBEDO =.80
ALBEDO ERROR %
55
50
45
40
35
30
25
20
15
10
5
0
1.0
0.9
0.8
0.7
0.6
0.5
0.4
0.3
0.2
0.1
COSINE (SOLAR ZENITH ANGLE)

Fig. 8

SURFACE ALBEDO

19 NOV 67

1223Z

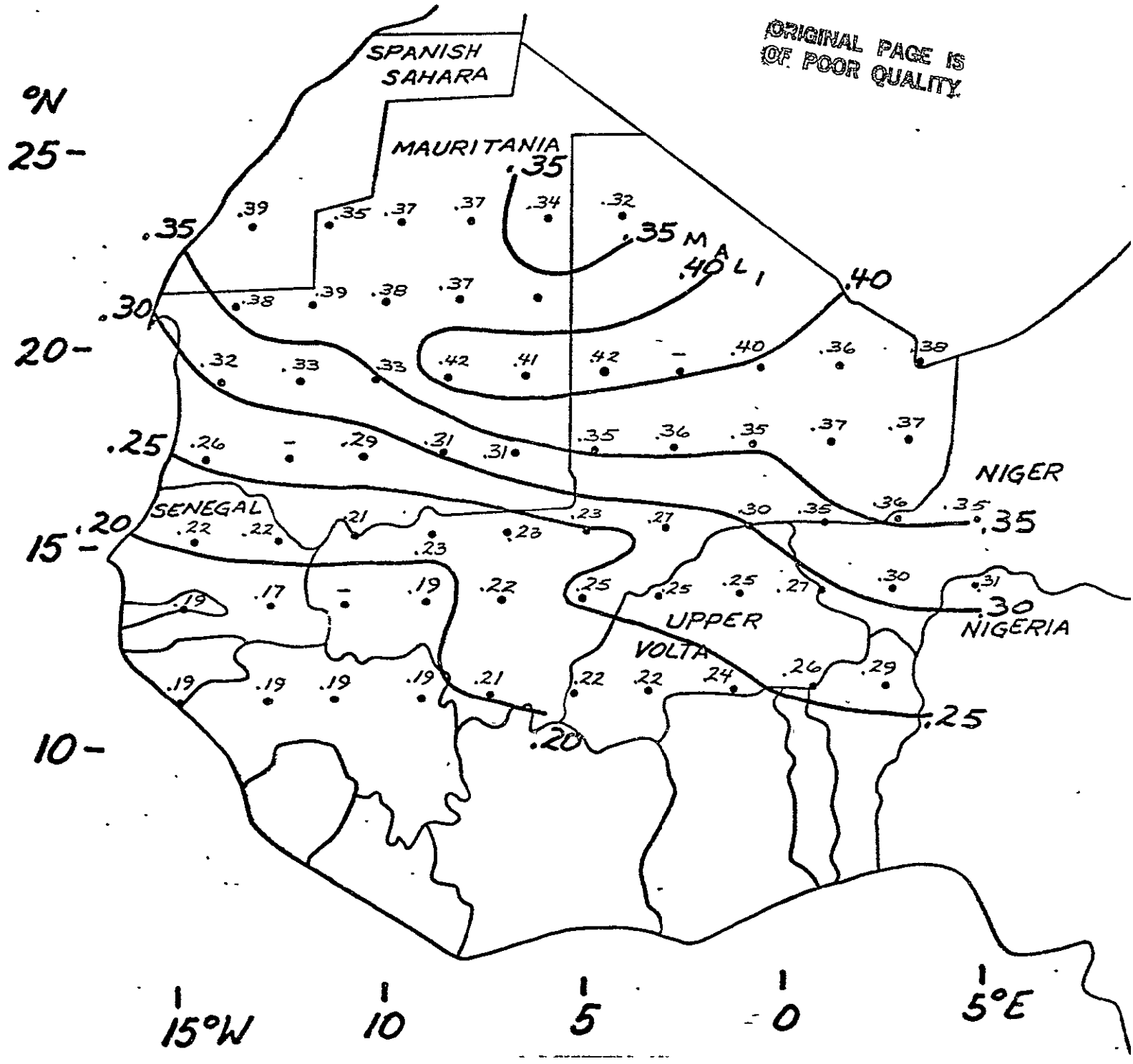

ORIGINAL PAGE IS OF POOR QUALITY

Fig. 9

SURFACE ALBEDO

15 SEPT 69

1424Z

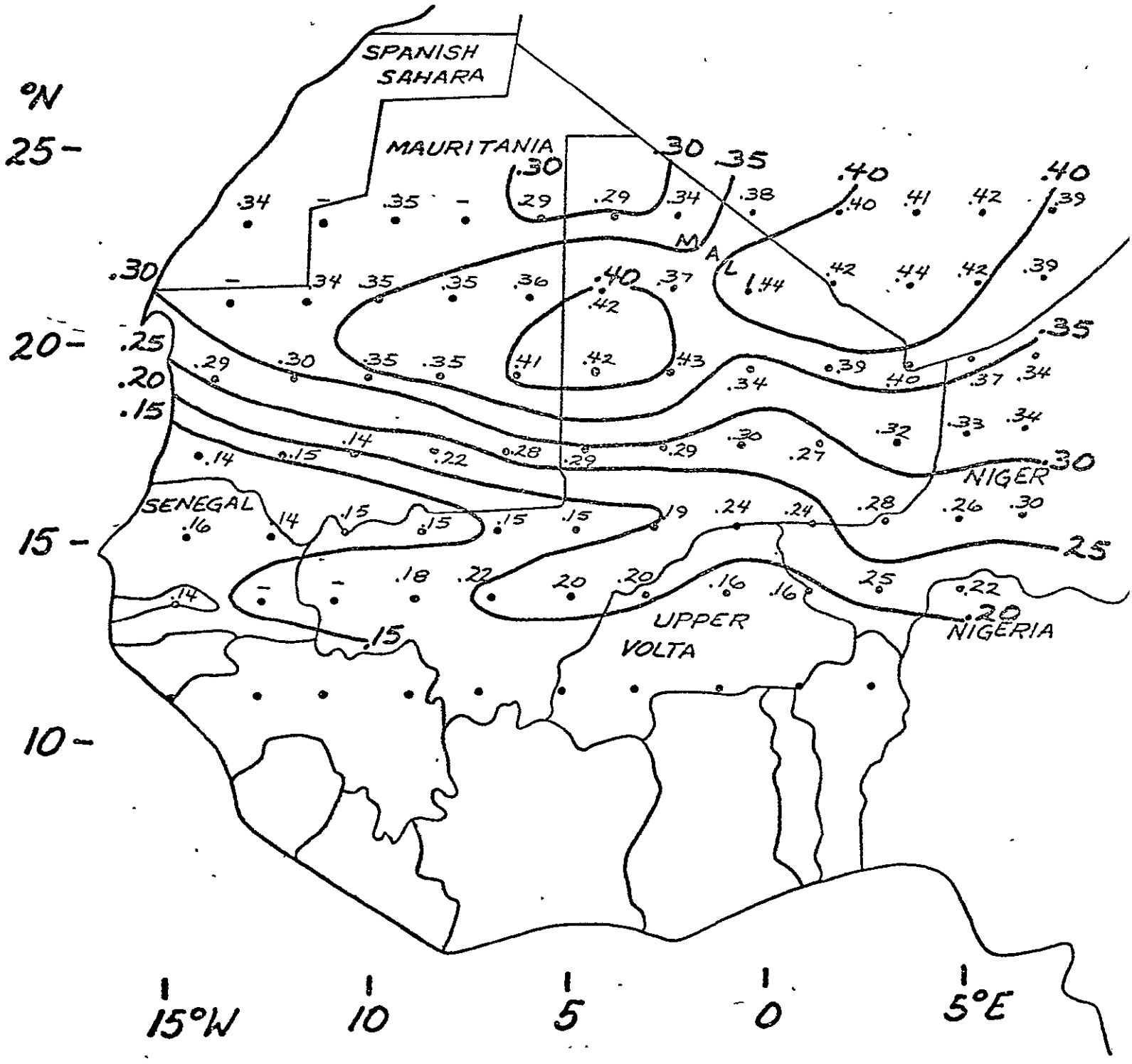

Fig. 10

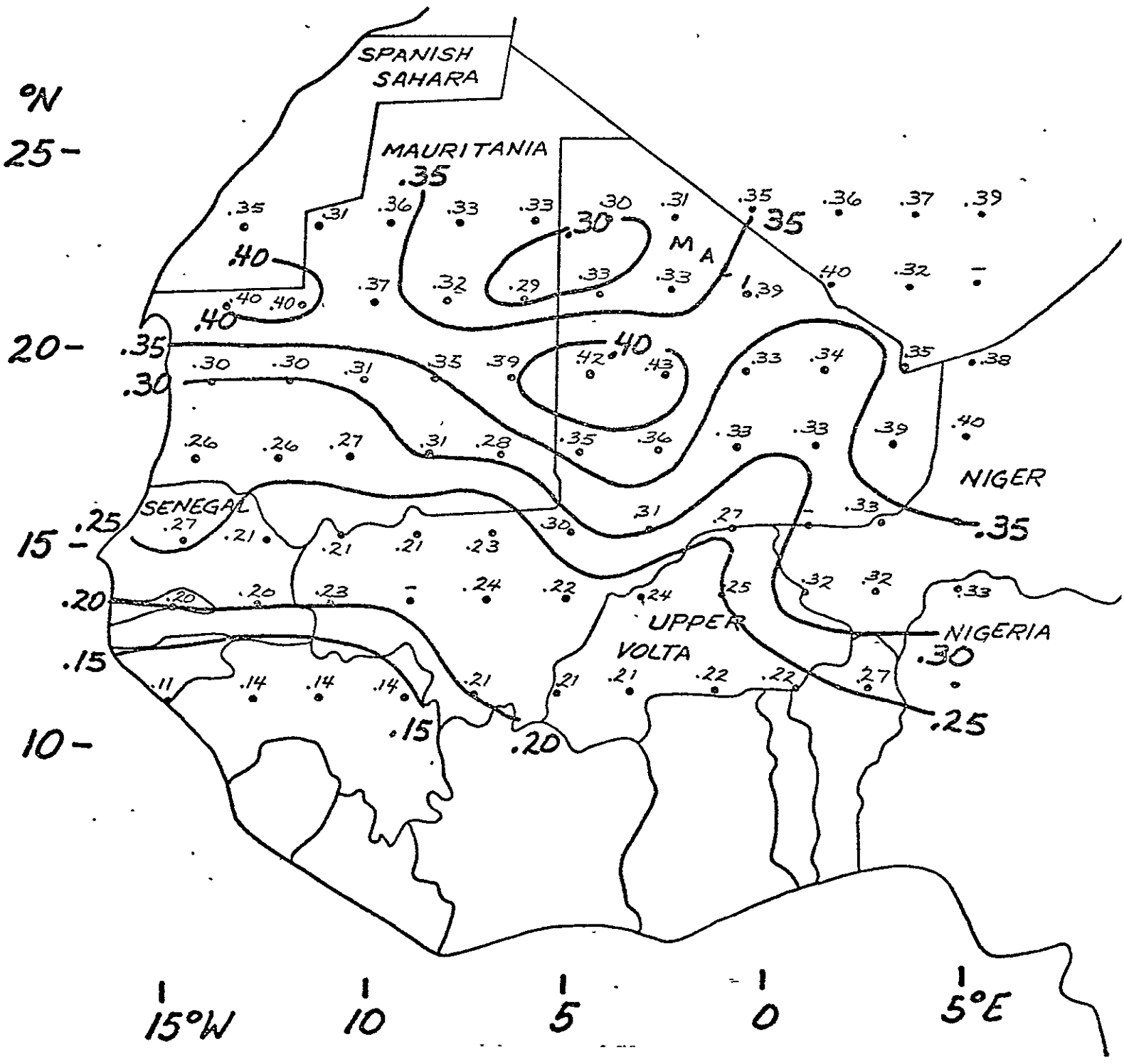
SURFACE ALBEDO
06 JAN 70
1442Z
SPANISH SAHARA
MAURITANIA
MALI
NIGER
NIGERIA
SENEGAL
UPPER VOLTA
°N
25-
20-
15-
10-
15°W
10
5
0
5°E

Fig. 11

SURFACE ALBEDO
19 JULY 72
1635Z

ORIGINAL PAGE IS
OF POOR QUALITY

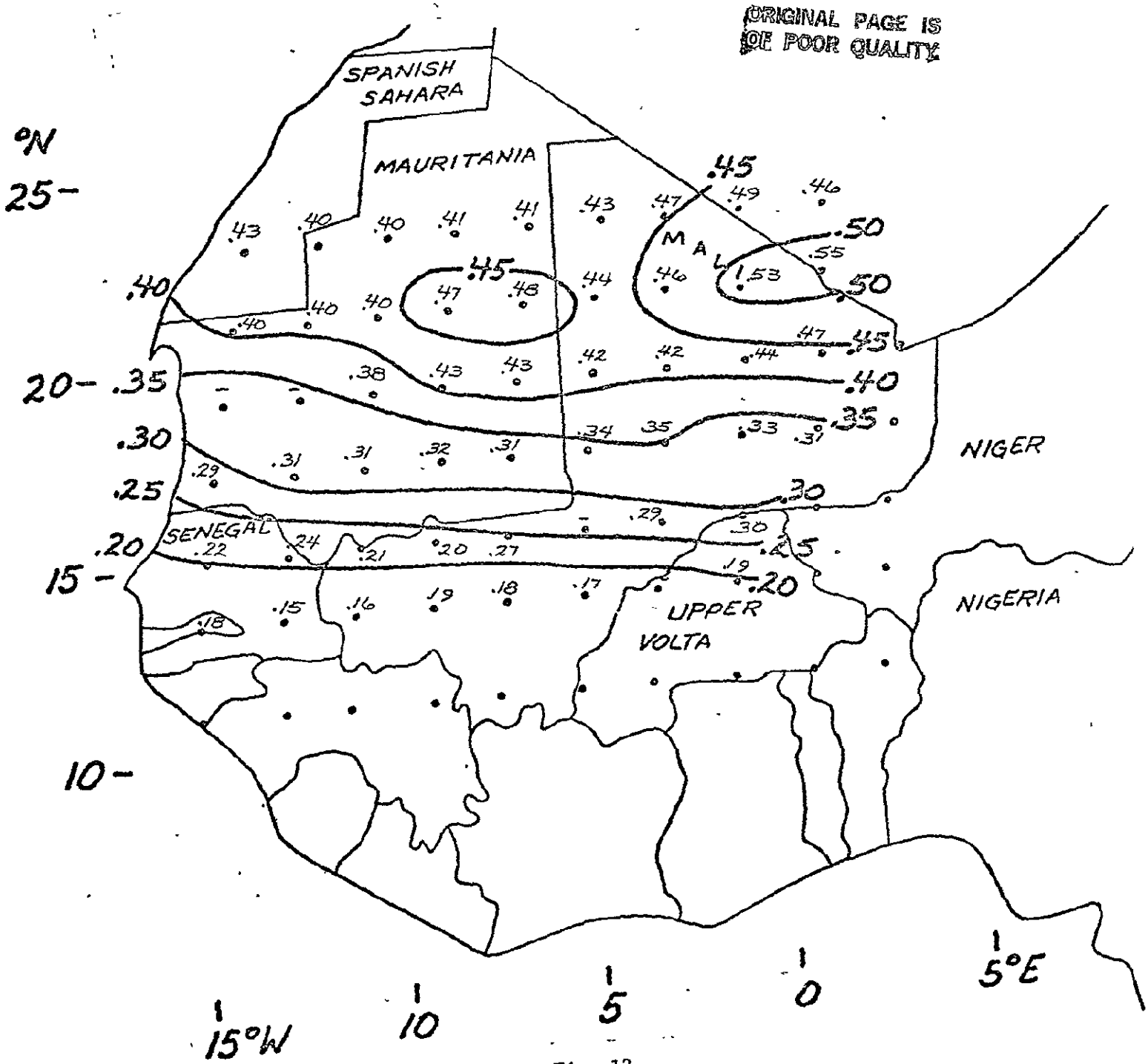

Fig. 12

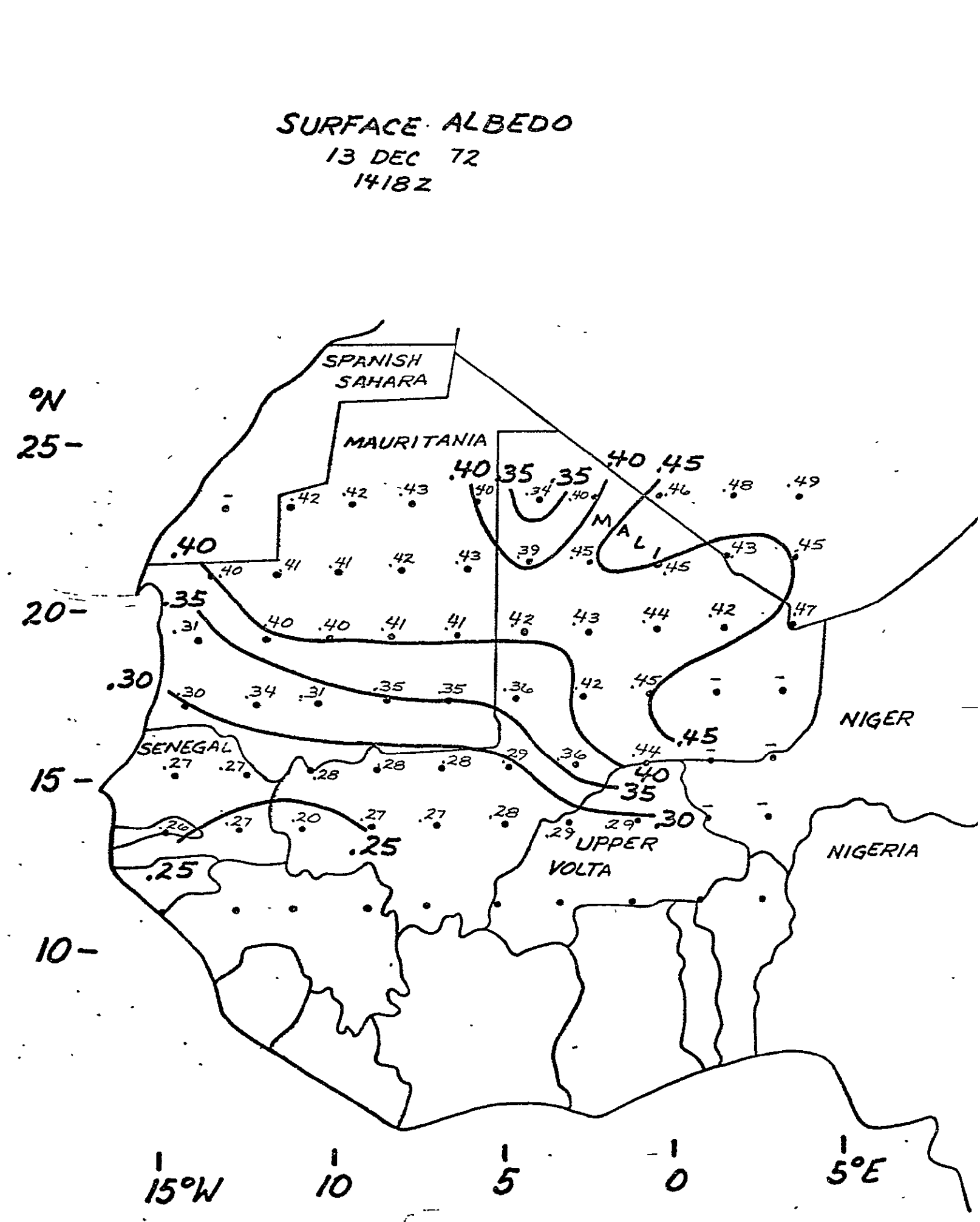
SURFACE ALBEDO
13 DEC 72
1418Z
SPANISH SAHARA
MAURITANIA
MALI
NIGER
SENEGAL
UPPER VOLTA
NIGERIA
°N
25
20
15
10
15°W
10
5
0
5°E

Fig. 13

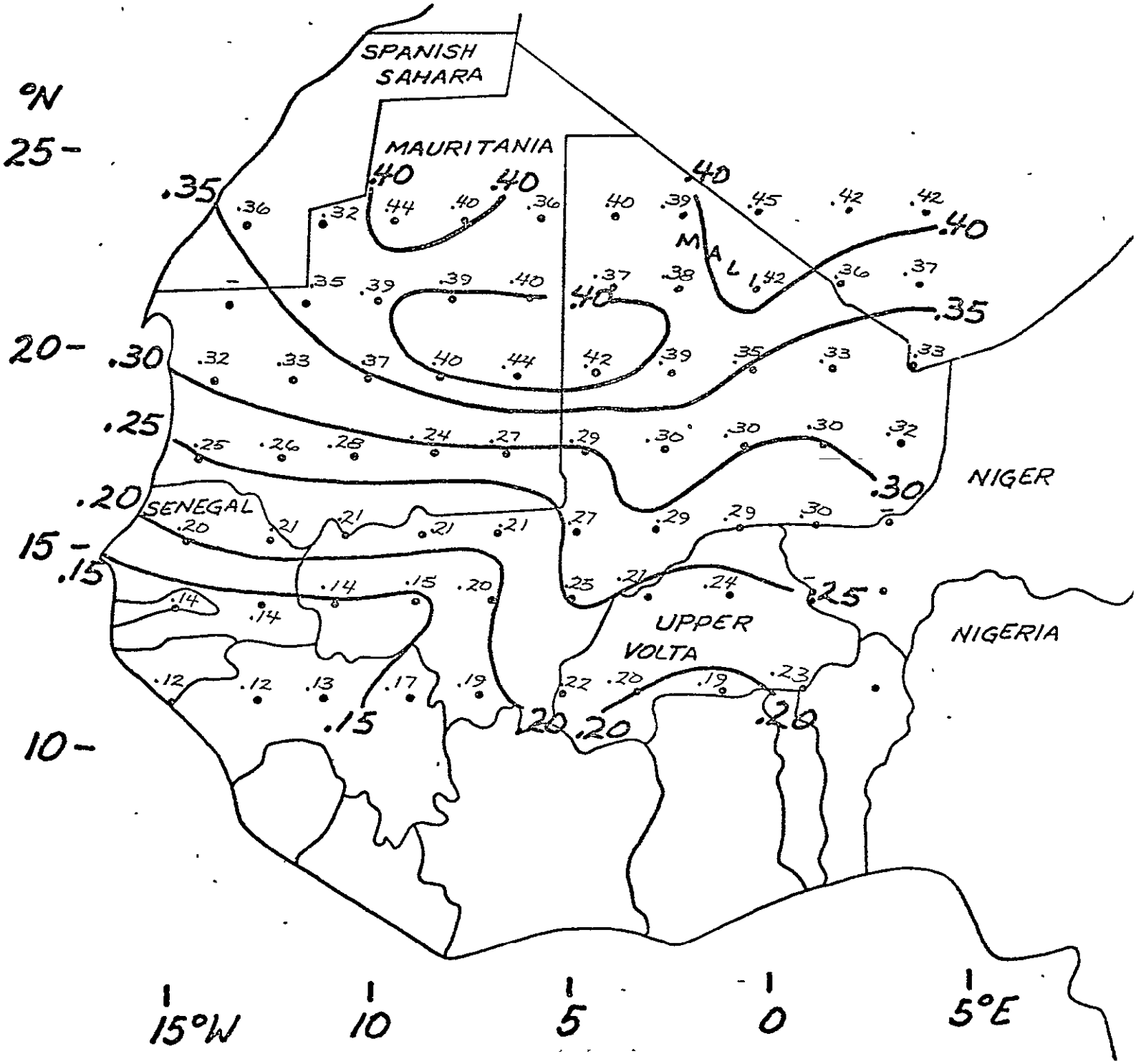
SURFACE ALBEDO
23 DEC 72
1252Z
SPANISH SAHARA
MAURITANIA
MALI
NIGER
SENEGAL
UPPER VOLTA
NIGERIA
°N
25-
20-
15-
10-
15°W
10
5
0
5°E

Fig. 14

SURFACE ALBEDO

14 AUG 73

1527Z

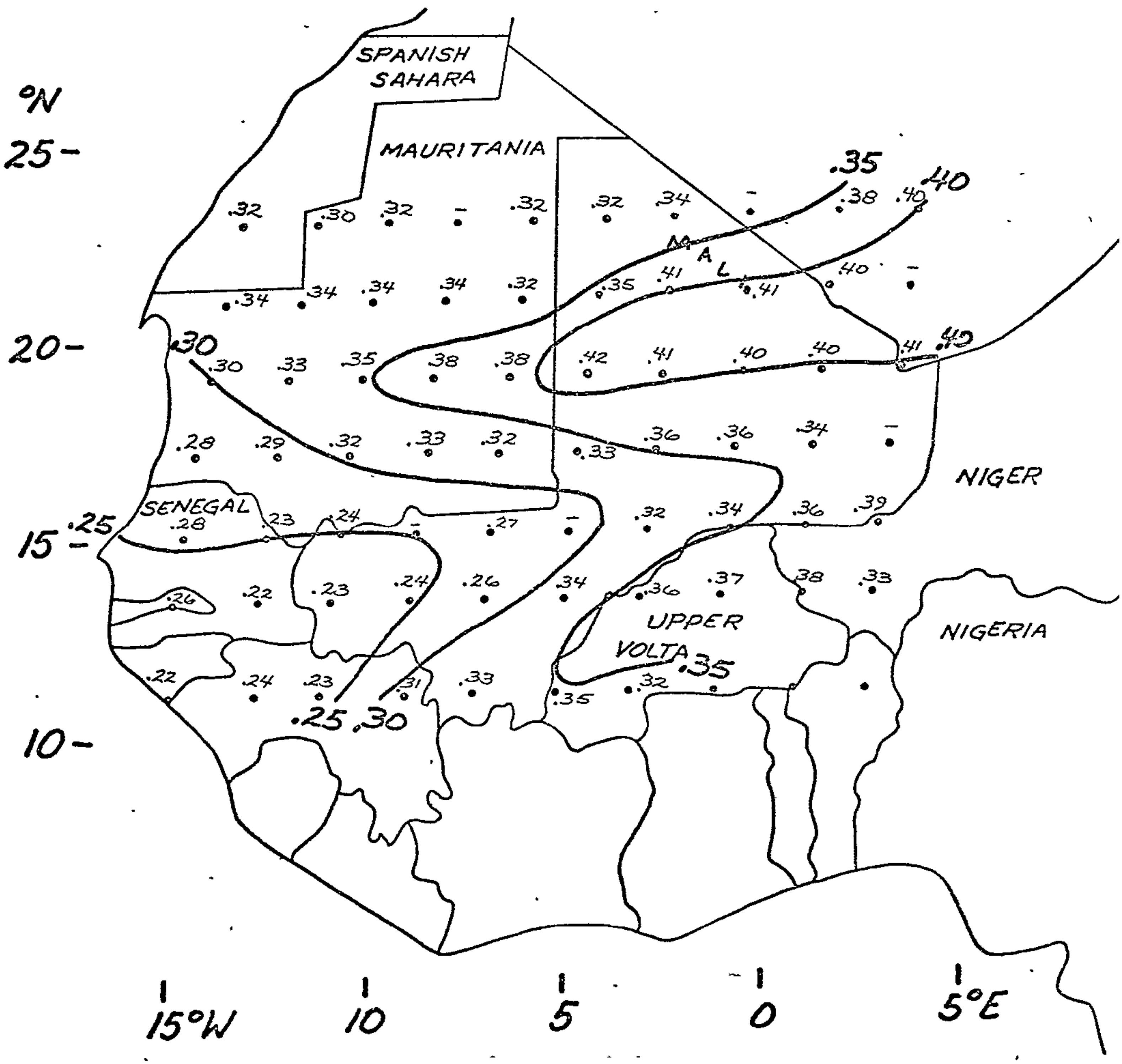

Fig. 15

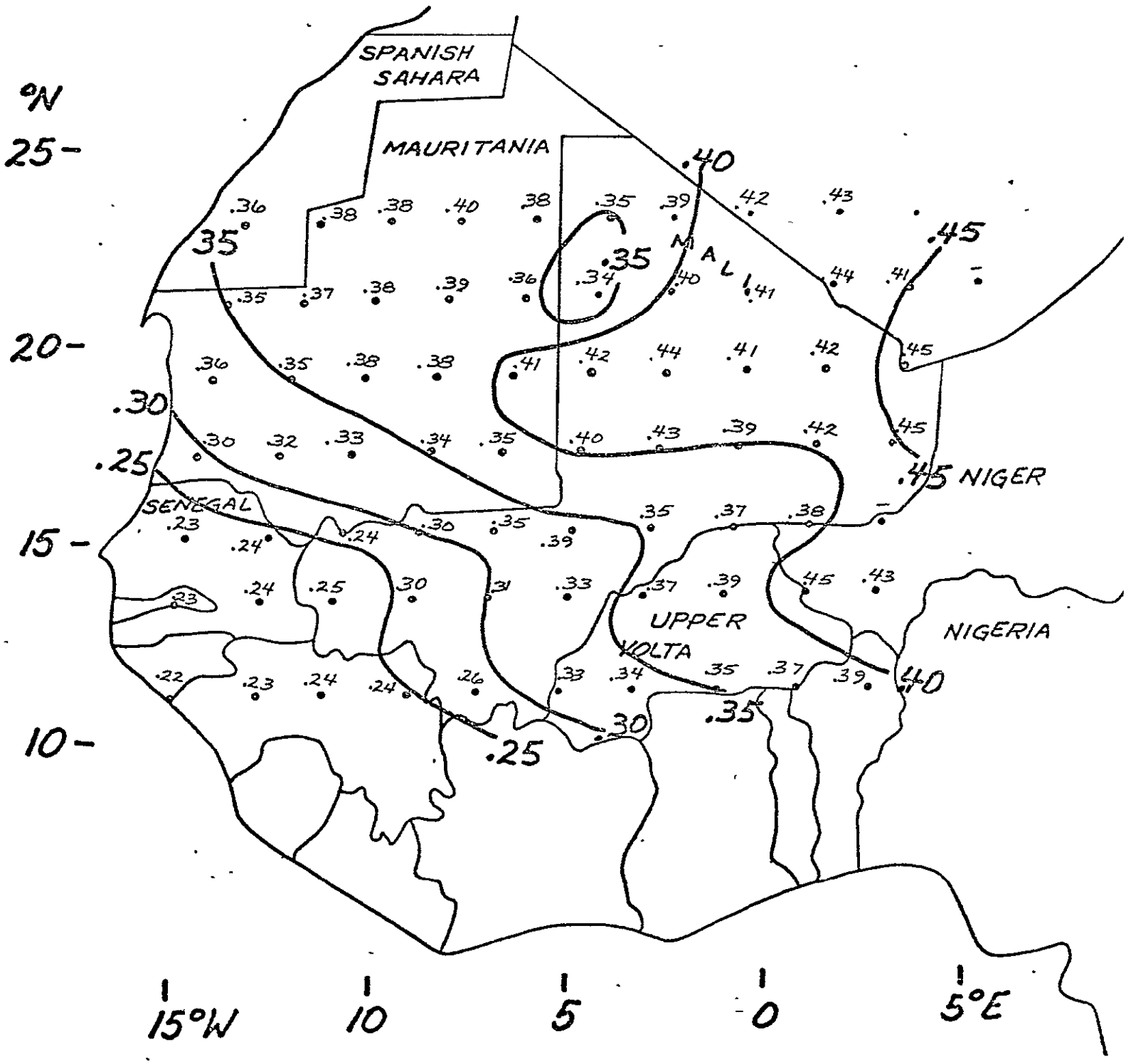
SURFACE ALBEDO
19 OCT 73
1556Z
SPANISH SAHARA
MAURITANIA
MALI
NIGER
SENEGAL
UPPER VOLTA
NIGERIA
°N
25-
20-
15-
10-
15°W
10
5
0
5°E

Fig. 16

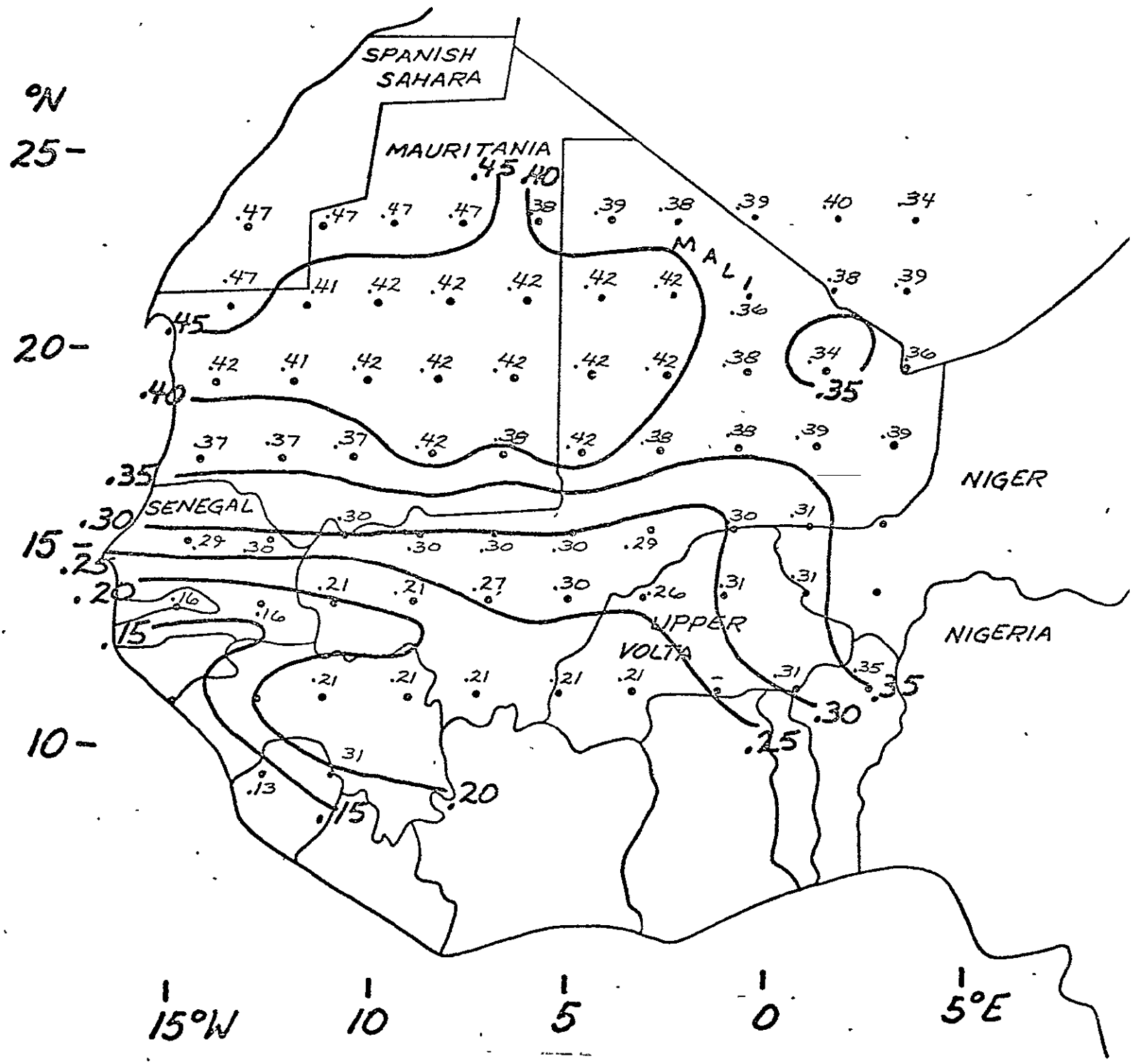
SURFACE ALBEDO
2 JULY 74
1304Z
SPANISH SAHARA
MAURITANIA
MALI
NIGER
SENEGAL
UPPER VOLTA
NIGERIA
°N
25-
20-
15-
10-
15°W
10
5
0
5°E

Fig. 17

SURFACE ALBEDO

21 SEPT 1974
1503Z

ORIGINAL PAGE IS
OF POOR QUALITY

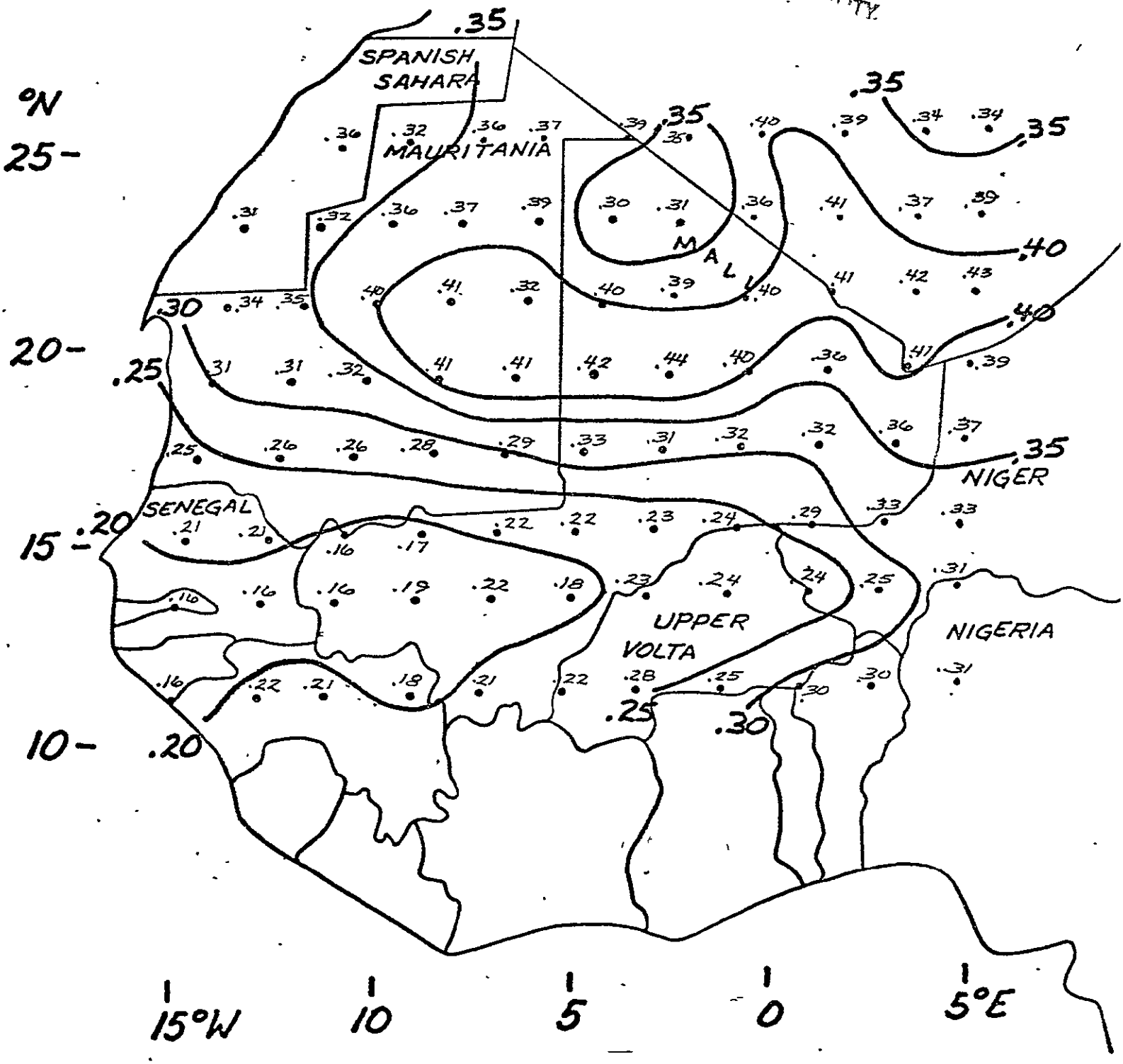

Fig. 18

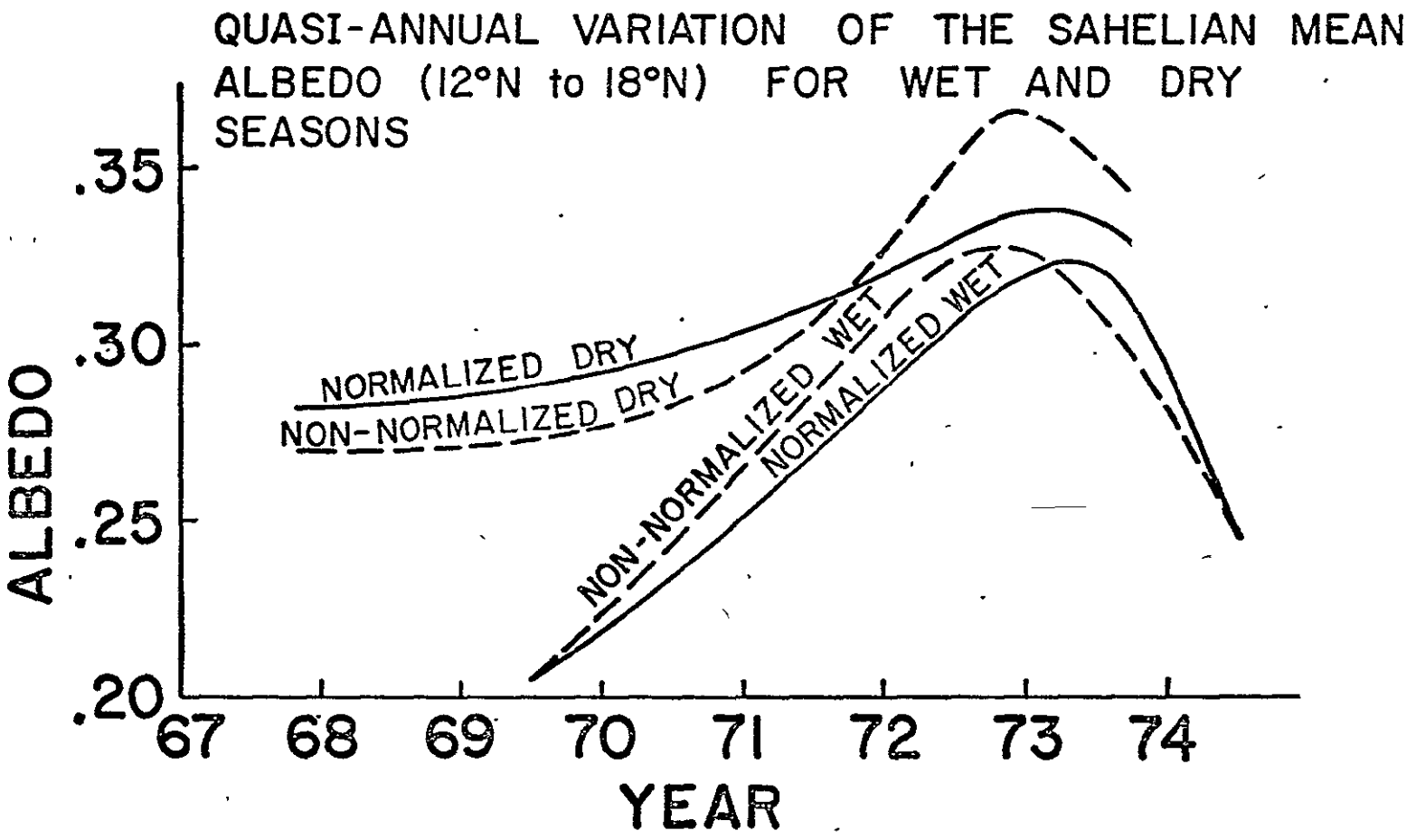
QUASI-ANNUAL VARIATION OF THE SAHELIAN MEAN ALBEDO (12°N to 18°N) FOR WET AND DRY SEASONS
ALBEDO
.35
.30
.25
.20
NORMALIZED DRY
NON-NORMALIZED DRY
NON-NORMALIZED WET
NORMALIZED WET
67
68
69
70
71
72
73
74
YEAR

Fig. 19

SEASONAL SURFACE ALBEDO CHANGE

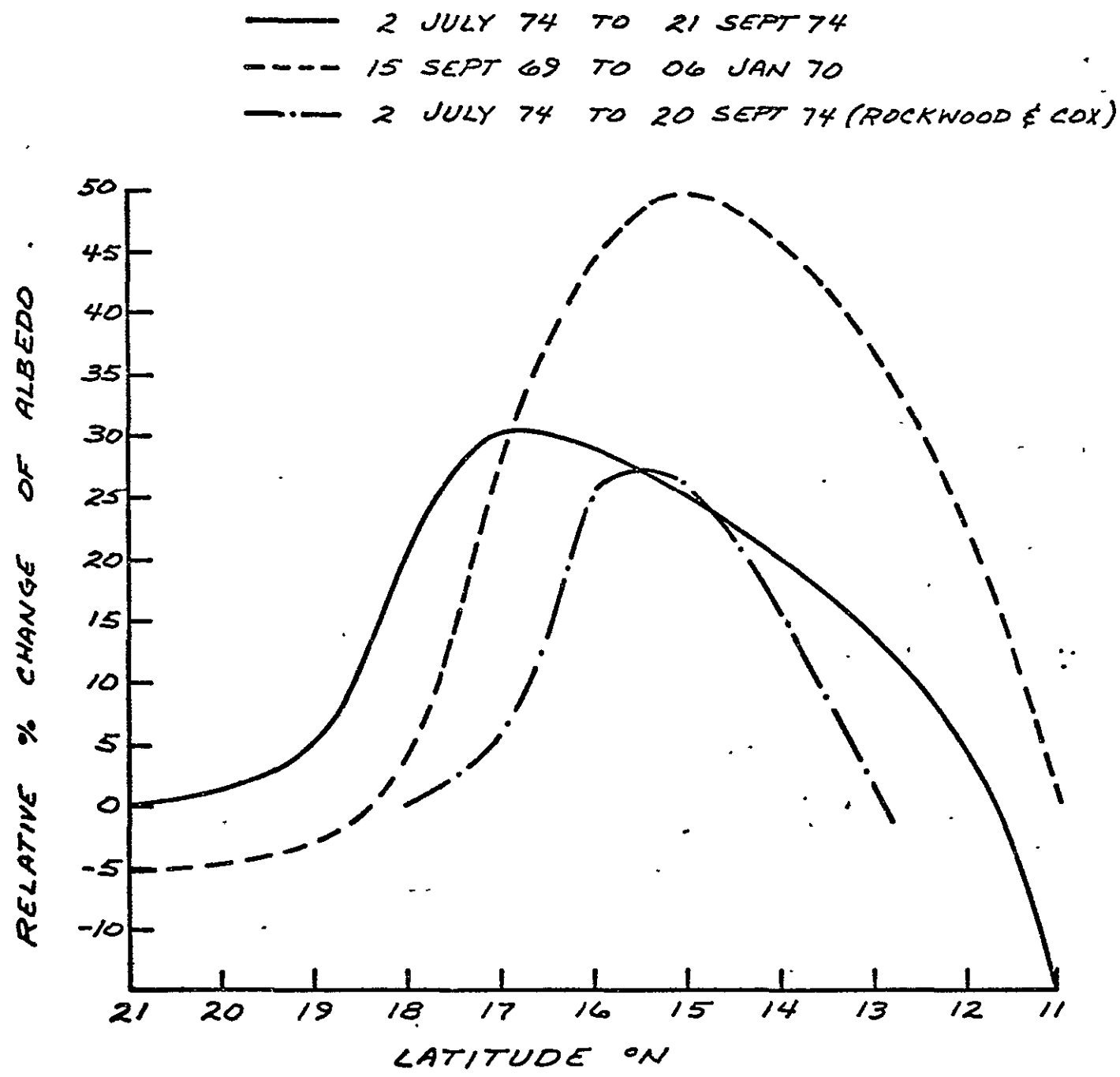

Fig. 20

SEASONAL SURFACE ALBEDO CHANGE

2 JULY 1974 TO 21 SEPT 1974

— % ALBEDO CHANGE = $\frac{\text{2 JULY} - \text{21 SEPT}}{\text{21 SEPT}} \times 100$

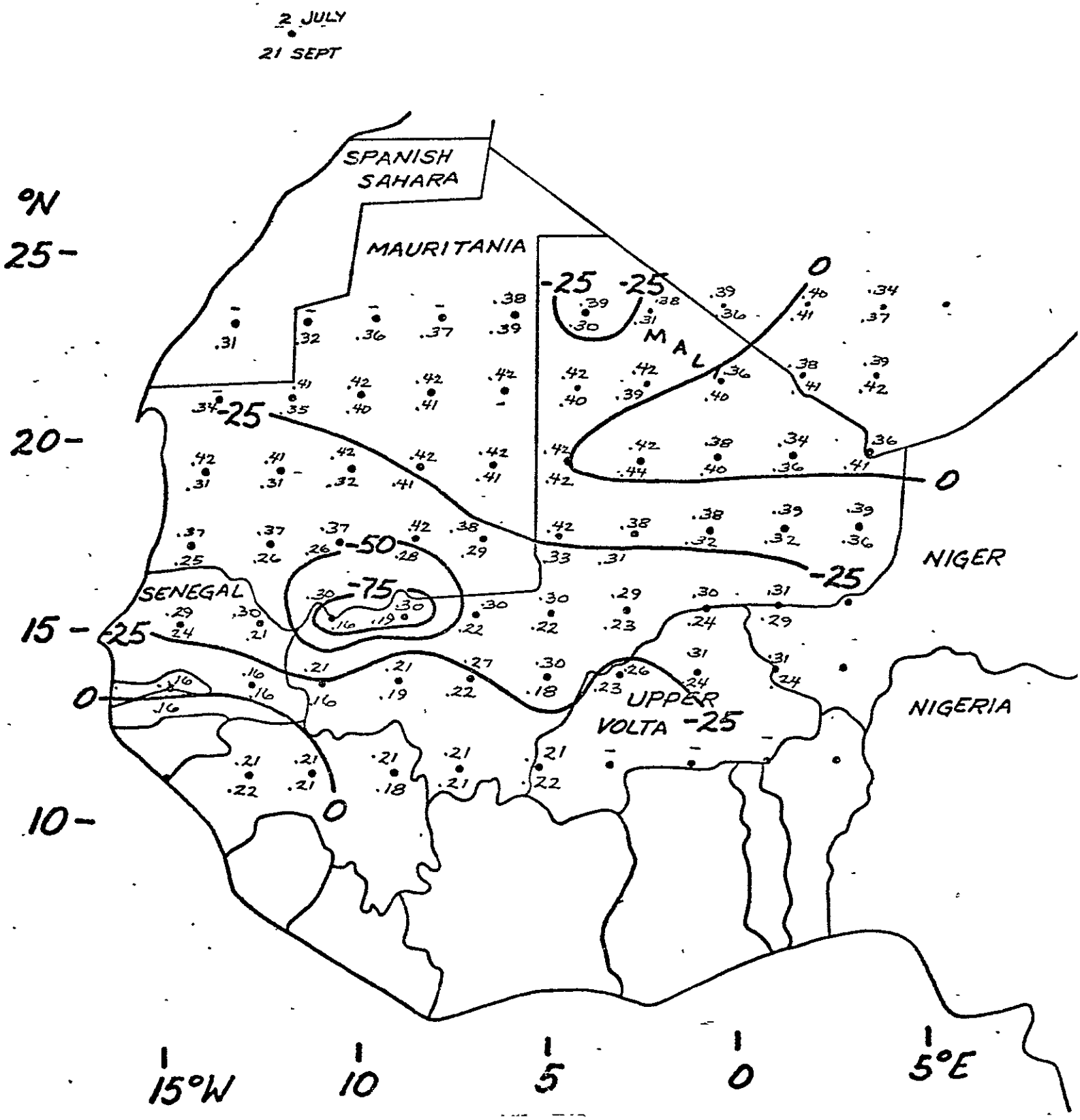

Fig. 21

SEASONAL SURFACE ALBEDO CHANGE

15 SEPT 1969 TO 06 JAN 1970

— % ALBEDO CHANGE = $\frac{\text{06 JAN} - \text{15 SEPT}}{\text{15 SEPT}} \times 100$

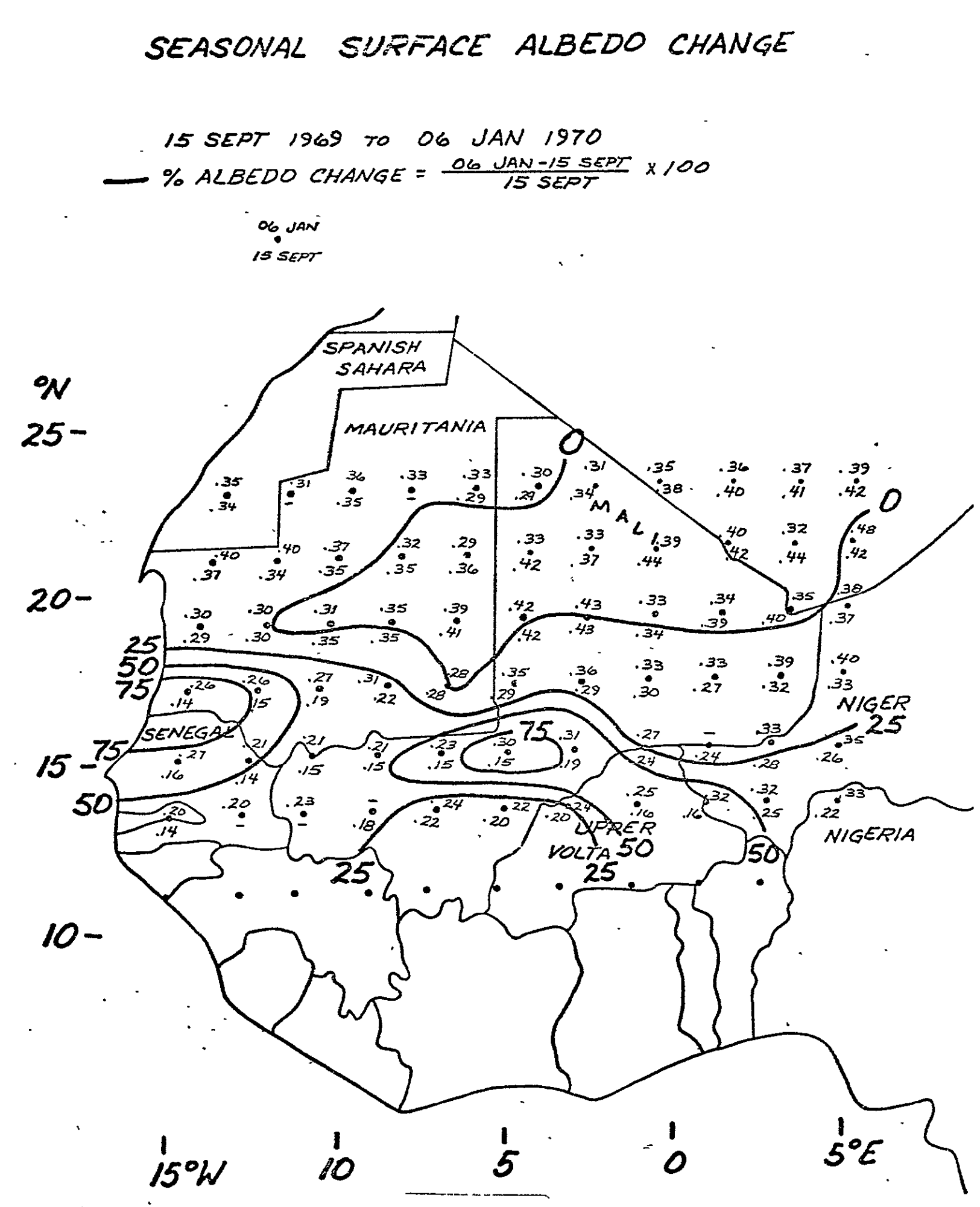

Fig. 22

SEASONAL SURFACE ALBEDO CHANGE

19 JULY 1972 TO 13 DEC 1972

— % ALBEDO CHANGE = $\frac{\text{13 DEC} - \text{19 JULY}}{\text{19 JULY}} \times 100$

13 DEC
19 JULY

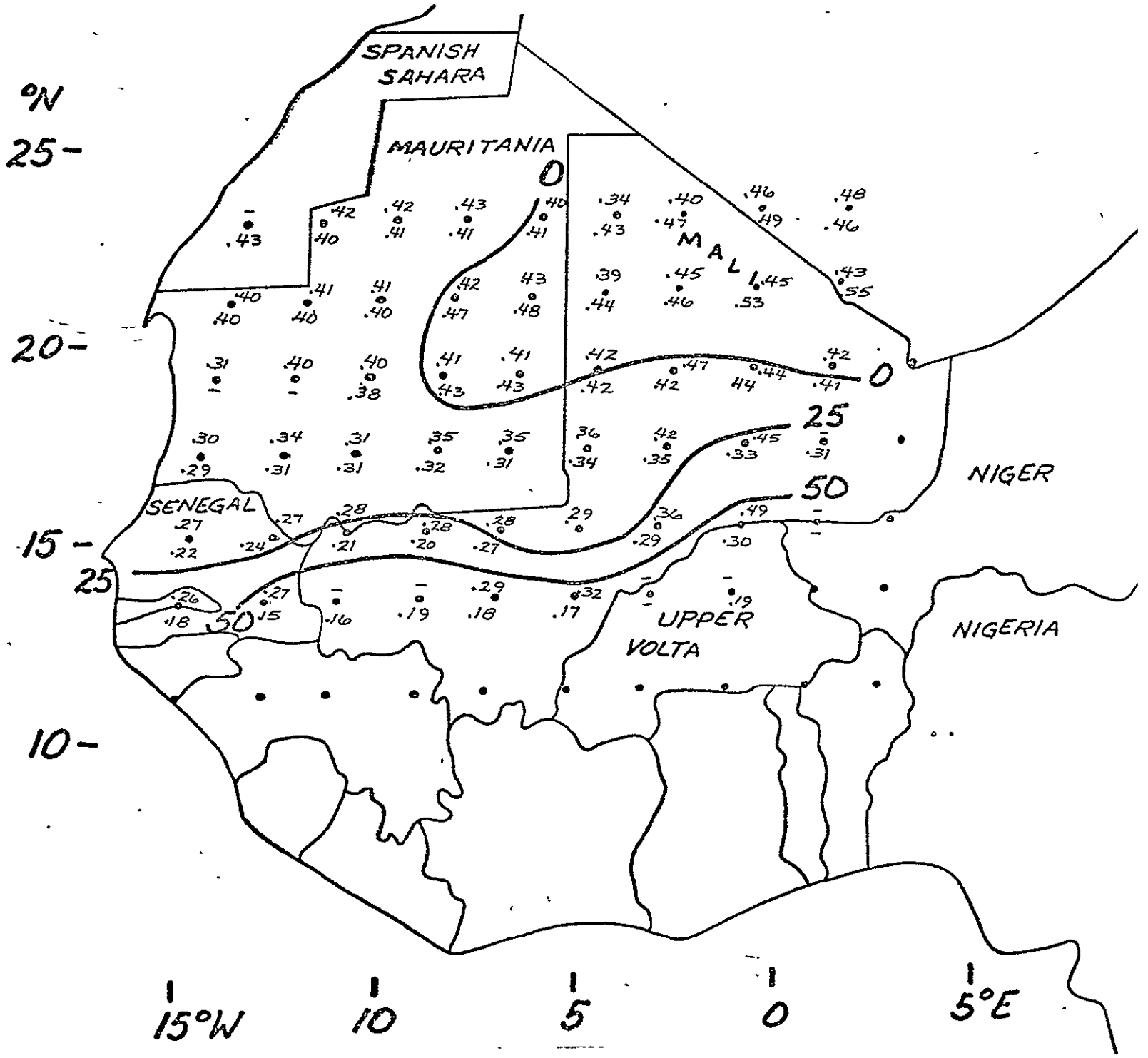

Fig. 23

SEASONAL SURFACE ALBEDO CHANGE

14 AUG 1973 TO 19 OCT 1973

—— % ALBEDO CHANGE = $\frac{\text{19 OCT} - \text{14 AUG}}{\text{14 AUG}} \times 100$

19 OCT
14 AUG

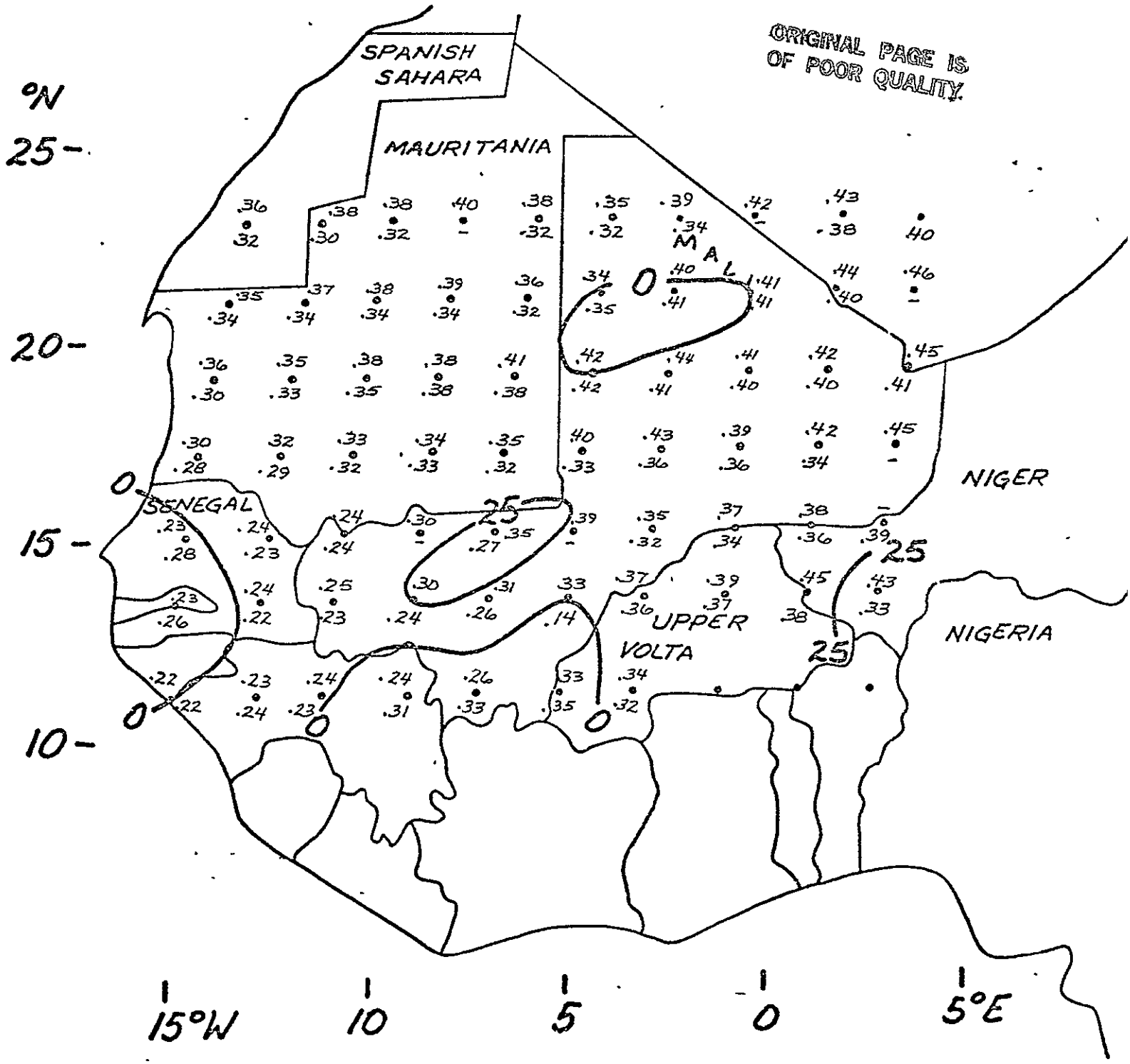

ORIGINAL PAGE IS OF POOR QUALITY

Fig. 24

ALBEDO CHANGE WET SEASON

15 SEPT 1969 TO 19 JULY 1972

—— % ALBEDO CHANGE = $\frac{\text{JULY 72} - \text{SEPT 69}}{\text{SEPT 69}} \times 100$

JULY 72
•
SEPT 69

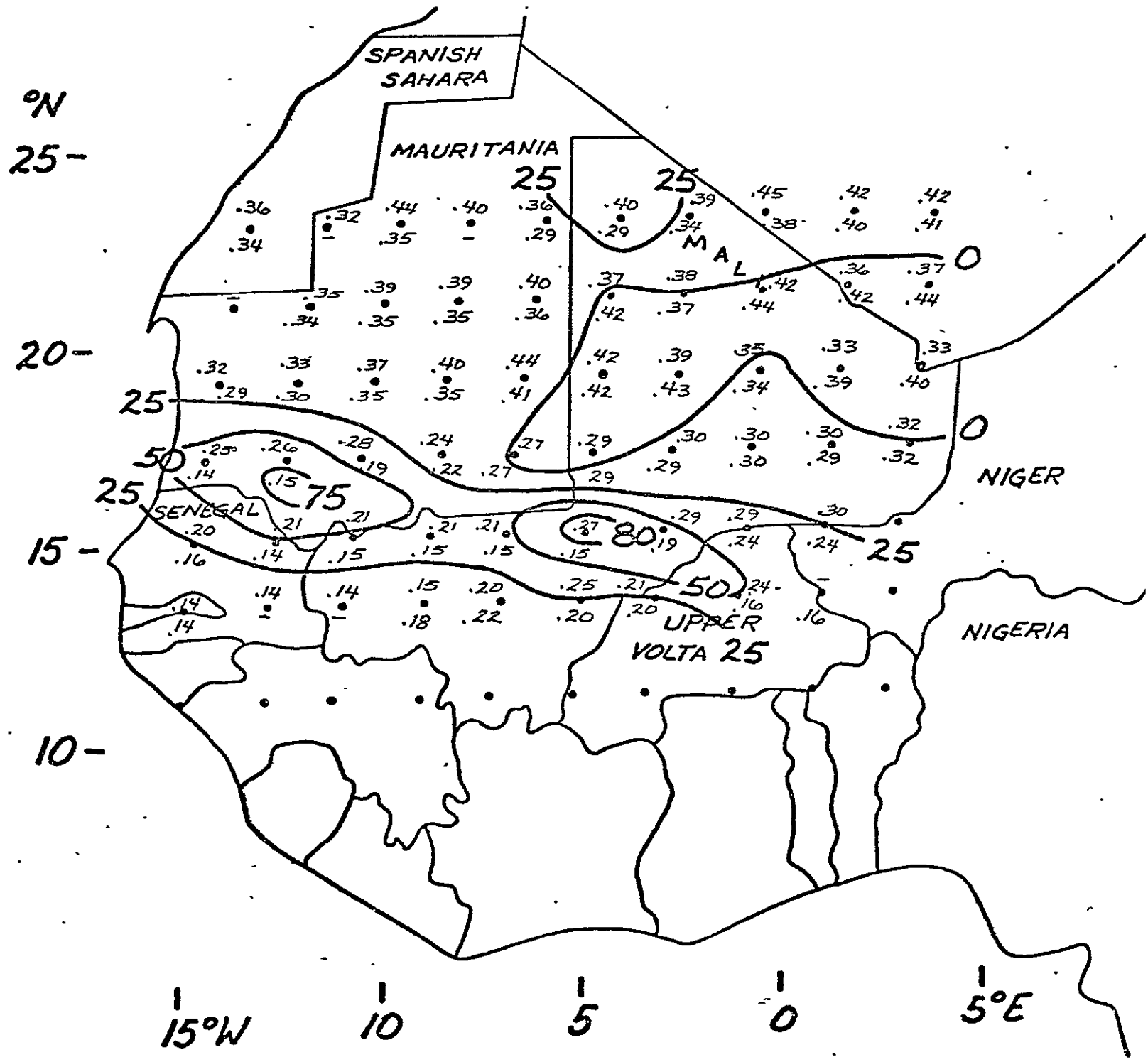

Fig. 25

ALBEDO CHANGE WET SEASON

15 SEPT 1969 TO 14 AUG 1973

— % ALBEDO CHANGE = $\frac{\text{AUG 73} - \text{SEPT 69}}{\text{SEPT 69}} \times 100$

AUG 73

SEPT 69

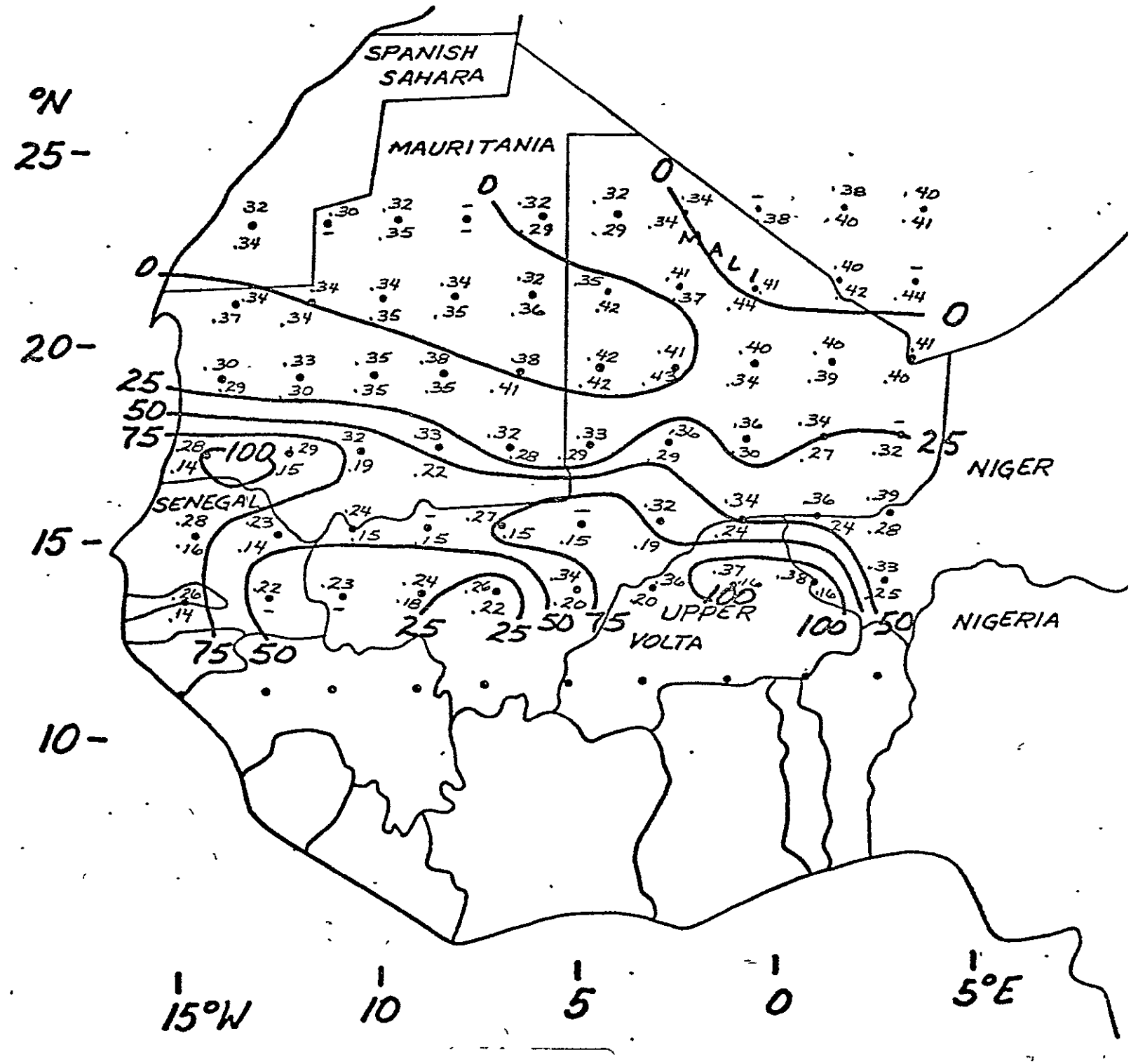

Fig. 26

ALBEDO CHANGE WET SEASON

15 SEPT 1969 TO 21 SEPT 1974

—— % ALBEDO CHANGE = $\frac{\text{SEPT 74} - \text{SEPT 69}}{\text{SEPT 69}} \times 100$

SEPT 74

SEPT 69

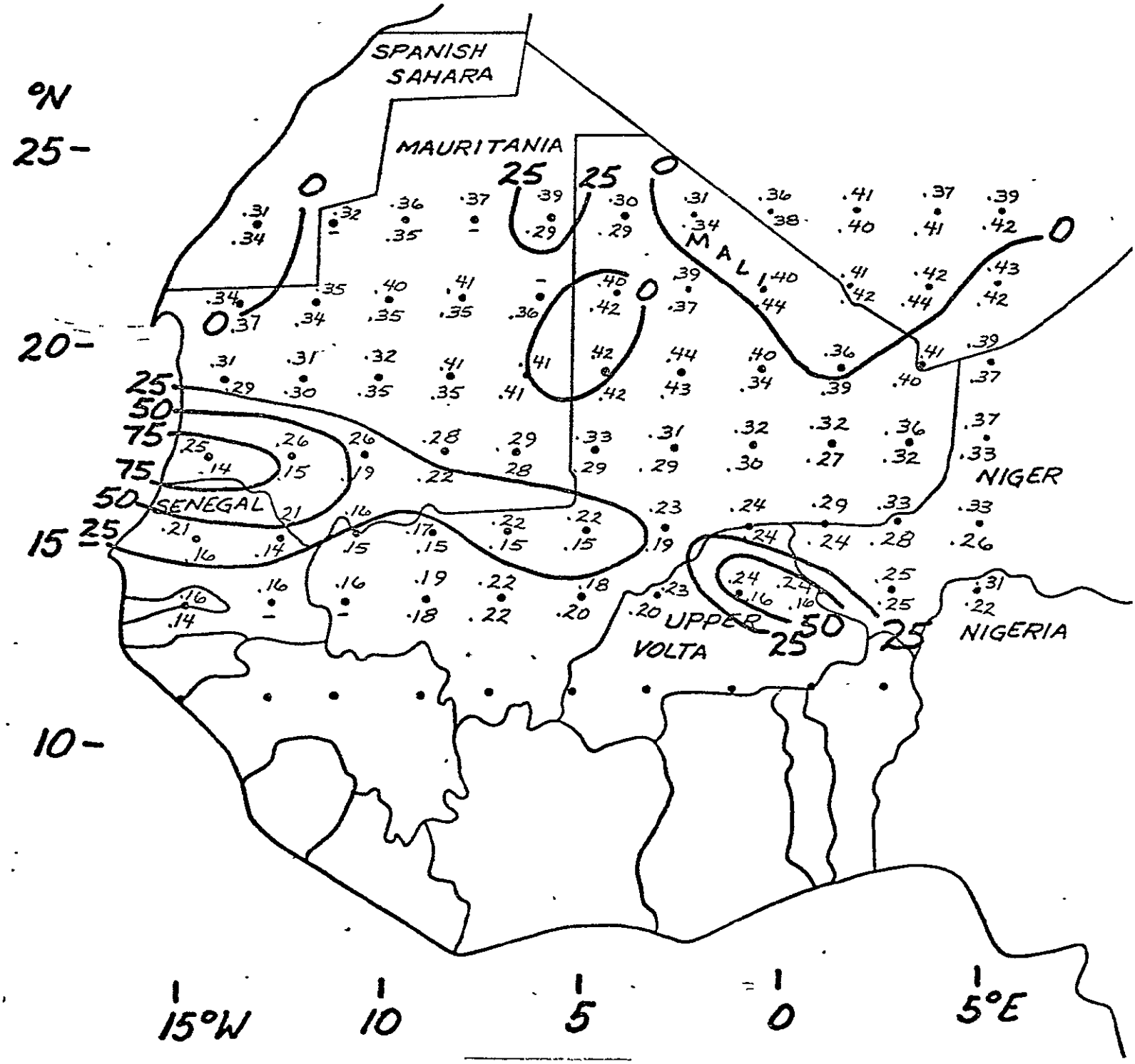

Fig. 27

ALBEDO CHANGE DRY SEASON

19 NOV 1967 TO 06 JAN 1970

— % ALBEDO CHANGE = $\frac{\text{JAN 70} - \text{NOV 67}}{\text{NOV 67}} \times 100$

JAN 70
•
NOV 67

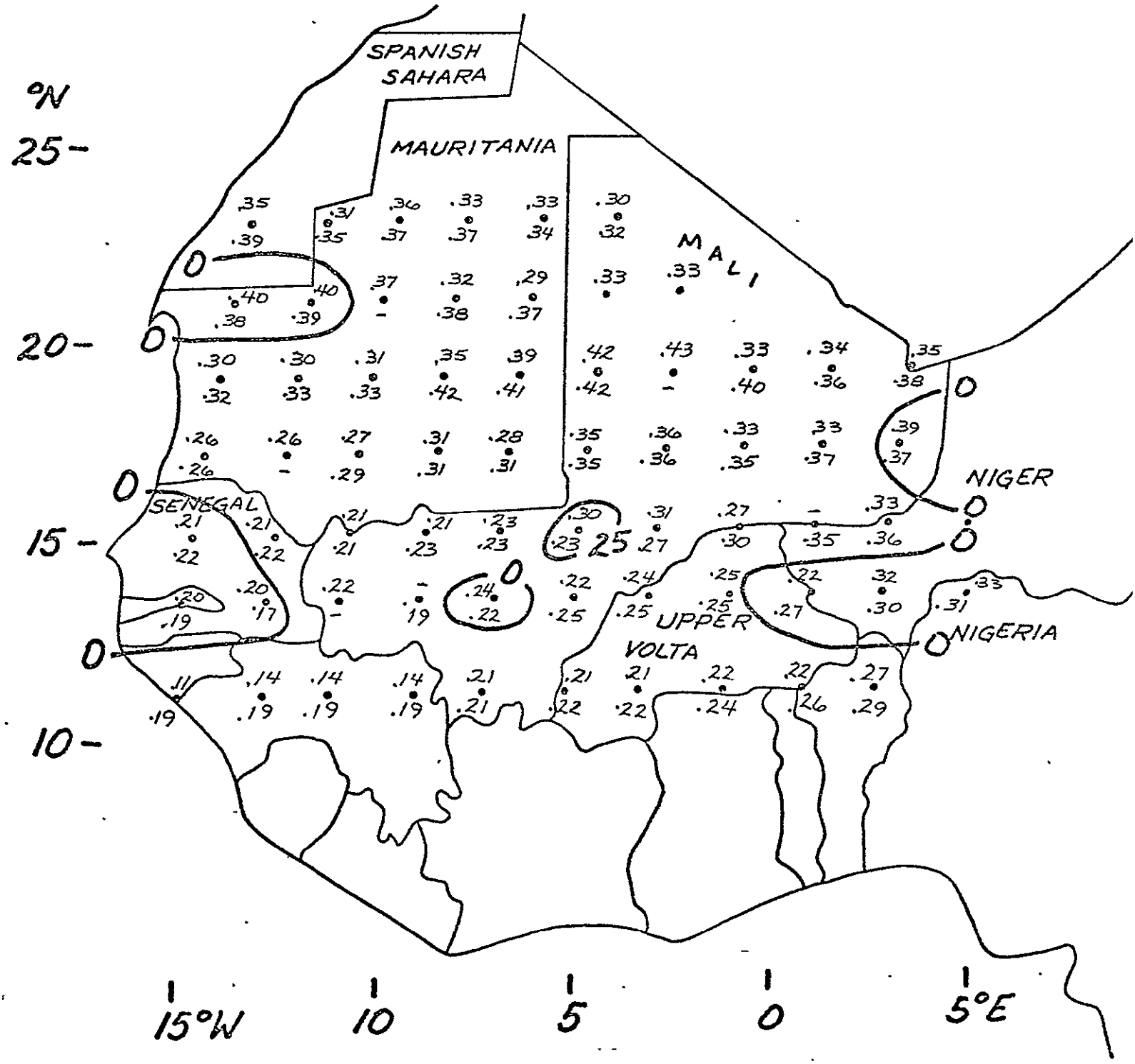

Fig. 28

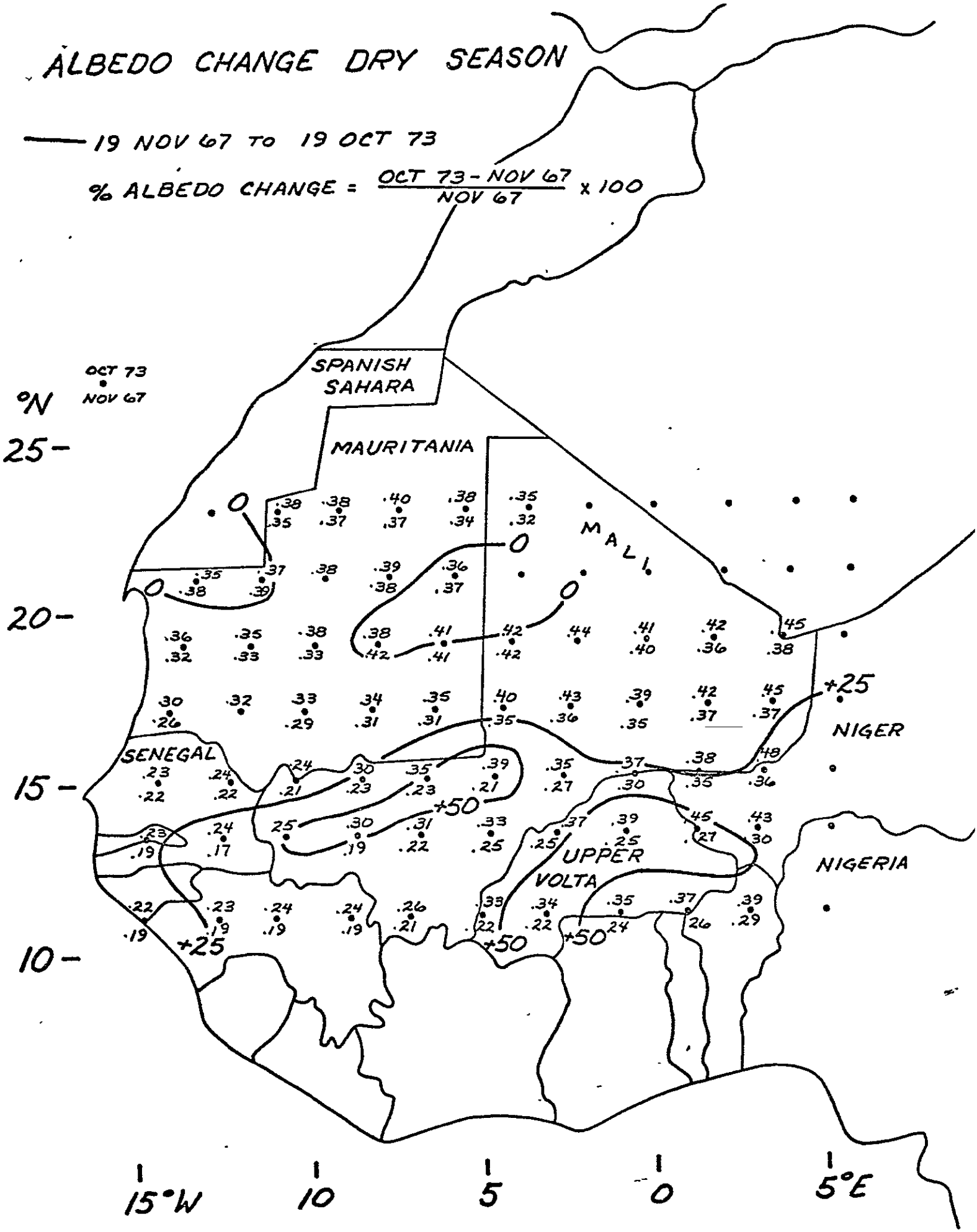
ALBEDO CHANGE DRY SEASON
19 NOV 67 TO 19 OCT 73
% ALBEDO CHANGE = OCT 73 - NOV 67 / NOV 67 x 100
OCT 73
NOV 67
°N
SPANISH SAHARA
MAURITANIA
MALI
NIGER
SENEGAL
UPPER VOLTA
NIGERIA
25-
20-
15-
10-
15°W
10
5
0
5°E

Fig. 29

ALBEDO CHANGE DRY SEASON

19 NOV 1967 TO 13 DEC 1972

— % ALBEDO CHANGE = $\frac{\text{DEC 72} - \text{NOV 67}}{\text{NOV 67}} \times 100$

DEC 72
•
NOV 67

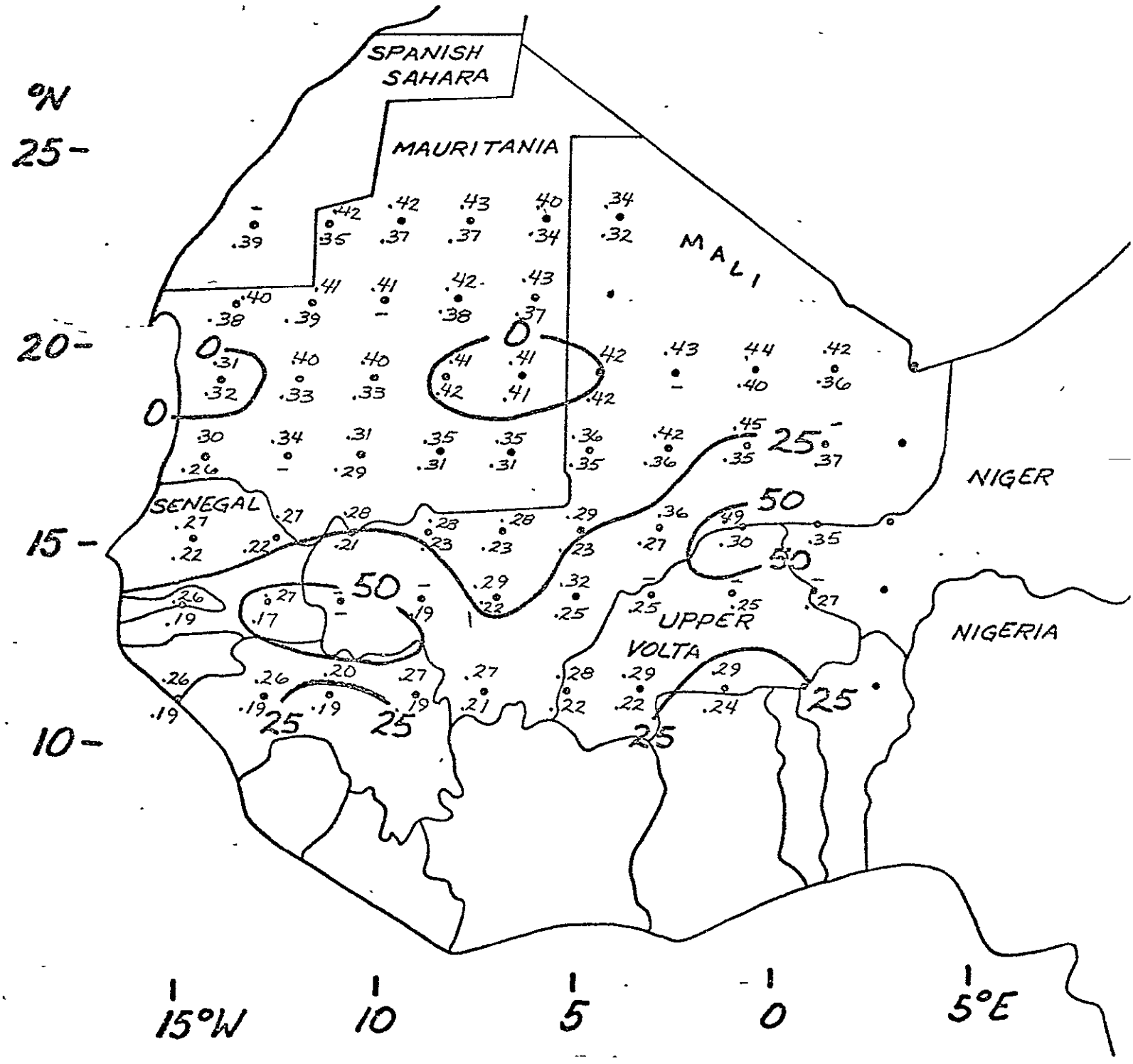

Fig. 30

ALBEDO CHANGE DRY SEASON

19 NOV 67 TO 2 JULY 74

$$\% \text{ ALBEDO CHANGE} = \frac{\text{JULY 74} - \text{NOV 67}}{\text{NOV 67}} \times 100$$

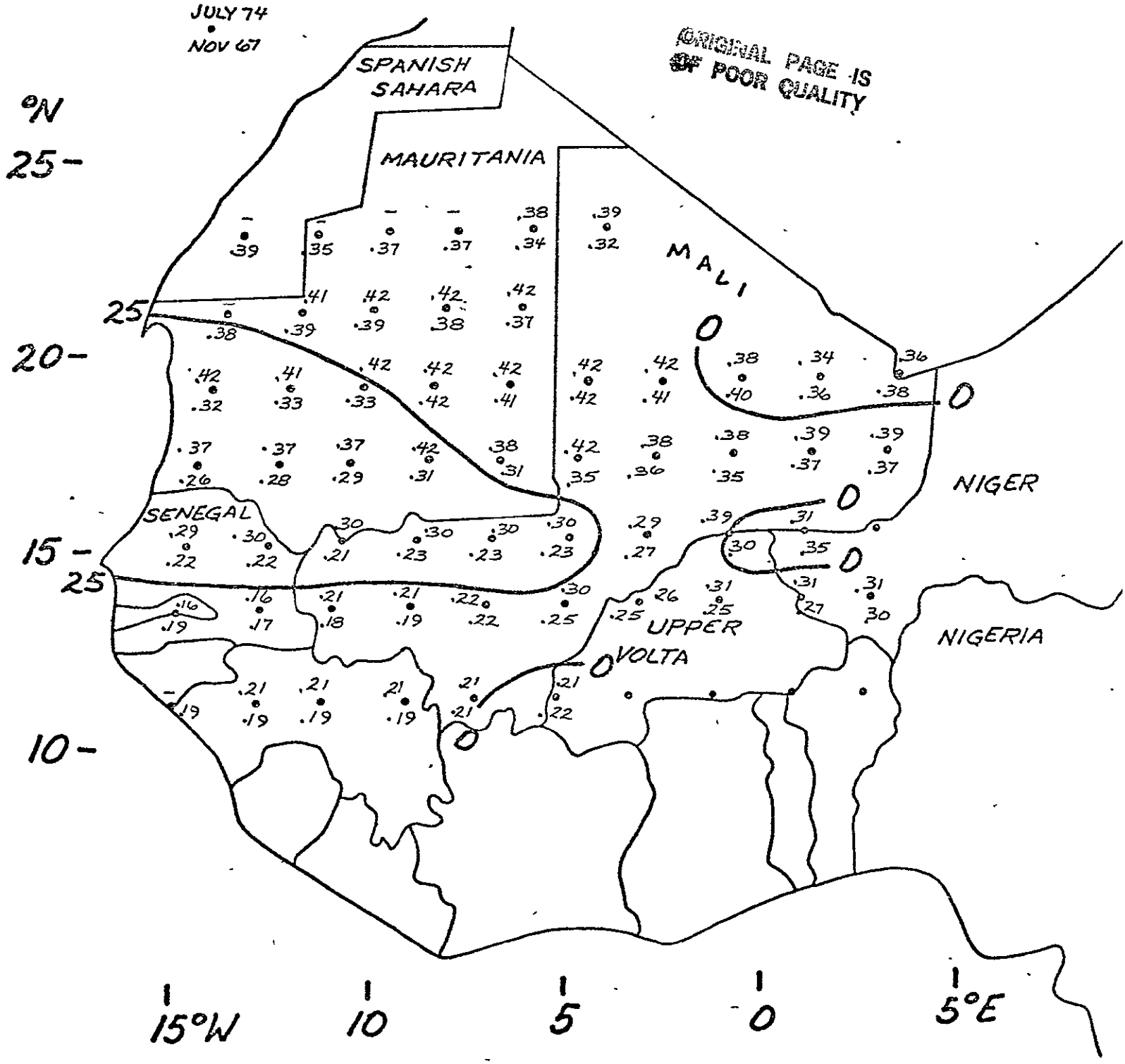

ORIGINAL PAGE IS OF POOR QUALITY

Fig. 31